



# UNIVERSITÀ DI PARMA

## ARCHIVIO DELLA RICERCA

University of Parma Research Repository

Dimensional analysis and calibration of a power model for compressive strength of solid-clay-brick masonry

This is the peer reviewed version of the following article:

*Original*

Dimensional analysis and calibration of a power model for compressive strength of solid-clay-brick masonry / Ferretti, D.. - In: ENGINEERING STRUCTURES. - ISSN 0141-0296. - 205:(2020), p. 110064. [10.1016/j.engstruct.2019.110064]

*Availability:*

This version is available at: 11381/2870648 since: 2021-01-04T18:18:36Z

*Publisher:*

Elsevier Ltd

*Published*

DOI:10.1016/j.engstruct.2019.110064

*Terms of use:*

Anyone can freely access the full text of works made available as "Open Access". Works made available

*Publisher copyright*

note finali coverpage

(Article begins on next page)

02 May 2026

# Dimensional analysis and calibration of a power model for compressive strength of solid-clay-brick masonry

Daniele Ferretti<sup>a,\*</sup>

<sup>a</sup>*Department of Engineering and Architecture, University of Parma, Viale delle Scienze 181/A, I 43124 Parma, Italy*

---

## Abstract

In the present work, the power model adopted to predict compressive strength of masonry as a function of brick and mortar strengths was studied by means of Dimensional Analysis, identifying the main dimensionless groups ruling the problem. The approach was applied on a dataset of solid-clay-brick masonry tests collected from the literature. Data were represented in a novel way that permitted to display the importance of the main dimensionless parameters. The dataset was filtered distinguishing these parameters and used to propose a new calibration of the power model considering mortar type and geometry of the specimens. Results show an interesting improvement in terms of indicators of regression quality with respect to the power models proposed in the literature. Both Dimensional Analysis and regressions confirm that the power models are specific for the type of specimens, i.e. dimensionless parameters, used for their calibration and direct comparisons among them should be done with great caution.

*Keywords:* A. Compressive strength, B. solid clay masonry, C. Eurocode 6, D. statistical analysis, E. dimensional analysis

---

## 1. Introduction

Forecasting masonry compressive strength as a function of geometrical and mechanical properties of its components is a challenging task that puzzled researchers since the beginning of twentieth century [1].

Usually, the compressive strength of masonry is determined as a function of brick and mortar strengths by means of: (a) tables [2] or phenomenological relationships [3, 4] calibrated by means of experimental data; (b) mechanical models based on linear/nonlinear behavior of mortar and bricks [5–8]; (c) nonlinear finite element models of wall specimens [9–13].

One of the most commonly adopted phenomenological relationship, which is frequently used as basis for comparison for new models, is the expression

$$f_M = K f_b^\alpha f_m^\beta \quad (1)$$

where  $f_M$  is the strength of masonry,  $f_b$  and  $f_m$  are the mean compressive strengths of bricks and mortars joints respectively, and  $K$ ,  $\alpha$ , and  $\beta$  are coefficients calibrated through the best fitting of a proper set of experimental data. Hereafter, subscripts  $M$ ,  $b$ , and  $m$  stand for masonry, brick, and mortar respectively, while Eq. (1) will be called “power equation” because of the exponents, or powers,  $\alpha$ , and  $\beta$ .

Several authors have calibrated the coefficients of the power equation by means of best fitting of experimental data with different types of bricks and blocks. A long list can be read in [14–16].

Although the method can be applied to any type of bricks, the present work concentrates on solid-clay-bricks, which are particularly common in existing masonry buildings, especially in monumental ones. Considering the related literature, it is mandatory to start from ENV1996-1-1 [17], briefly EC6, which provides an expression for the compressive strength of new masonry walls. For this reason, the power equation is also called “EC6-like” equation. The coefficient  $K$  varies between 0.4 and 0.7 depending on the brick types and construction details, such as thickness of bed joints, presence of head joints, and thickness of

29 the wall. Furthermore, the formula is valid for  $f_b < 75$  MPa,  $f_m < 20$  MPa, and  
 30  $f_m < 2f_b$  if the units are laid on general-purpose mortar. In case of multi-leaf  
 31 walls, the strength is multiplied by the coefficient 0.8. Malek [18] and Hendry  
 32 and Malek [19] analyzed full-scale story-height brickwork walls and observed  
 33 that the coefficients are sensitive to the wall thickness (102.5 and 215 mm) and  
 34 to the mortar type. Lumantarna et al. [20] calibrated the equation using both  
 35 New Zealand historical field-extracted and laboratory-constructed three-brick  
 36 high prisms composed of historical clay bricks and mortar. Mann [21] analyzed  
 37 925 specimens with bricks of different typologies (aerated concrete, lightweight  
 38 concrete, sandstone, and solid clay). Kaushik et al. [22] fitted the results of 17  
 39 specimens (5 stacked bond bricks) in solid clay. Gumaste et al. [23] studied In-  
 40 dian stack-bonded prisms characterized by solid-clay-bricks that were relatively  
 41 softer than mortar. Also Dayaratnam [24] studied specimens of Indian masonry.

42 Table 1 shows the coefficients proposed by the aforementioned authors. For  
 43 EC6 [17] the values of solid clay units (group 1), general-purpose mortar, and  
 44 single-wythe masonry have been written. For Hendry and Malek [19], the co-  
 45 efficients for walls with thickness  $t_M = 102.5$  mm have been reported. All  
 46 the expressions considered provide the mean compressive strength except EC6,  
 47 which deals with the characteristic one.

48 In addition, Table 1 shows the values of the coefficient of determination  $R^2$   
 49 declared by the authors, when available, which allows a concise judgment about  
 50 the quality of the best fittings, i.e. a measure of the scatter between the values  
 51 predicted by the formula and the experimental data. The closer the value of  $R^2$   
 52 comes to 1, the better is the approximation.

53 The values of  $R^2$  have not been published for all the considered cases and  
 54 the confidence intervals of the coefficients are not available. Without these data,  
 55 it is impossible comparing the accuracy of the formulae. Furthermore, it can  
 56 be noticed that the coefficients proposed by the authors are quite different:  $K$   
 57 goes from 0.28 to 0.83 and  $\alpha$  from 0.49 to 0.85. This is due to the inevitable  
 58 statistical dispersion of the experimental results, as well as to the different types  
 59 of specimens analyzed.

60 To compare the models proposed by the cited authors, the equations are  
61 plotted in Fig. 1 for mortar strengths  $f_m$  equal to 1.0 MPa and 10.0 MPa. As can  
62 be seen, the curves are quite dispersed. Small variations of the coefficients cause  
63 very different predictions. For instance, for a mortar strength  $f_m = 1.0$  MPa  
64 and bricks with compressive strength  $f_b = 15$  MPa, which are typical values for  
65 an historical masonry made with solid-clay-bricks and aerial lime mortar, the  
66 equations predict a masonry strength ranging from 1.0 to 5.7 MPa (Fig. 1a).  
67 The degree of uncertainty is very important. For the same masonry type, a  
68 table in the Italian code standard [2] recommends a value within the range of  
69 2.6 to 4.3 MPa, regardless of mortar and brick strengths.

70 For more accurate predictions, the choice of a suitable formula is necessary.  
71 Aims of the present work are: (a) understand advantages and limits of the power  
72 models; (b) find which power model proposed in the literature is more suitable  
73 to forecast the strength of masonry built with solid-clay-bricks; (c) understand  
74 if the models proposed for general-purpose mortar are also valid in the case of  
75 lime mortar (which is particularly important for historical buildings but also  
76 for new ones made with lime mortar); (d) propose a new calibration specific  
77 for solid-clay-brick masonry considering also the mortar type; (e) discuss the  
78 quality of fitting and quantify the errors on the predicted strengths.

79 To this purpose, the structure of the power equation was here interpreted,  
80 probably for the first time, by means of Dimensional Analysis. The role of the  
81 different parameters affecting the compressive strength (e.g. the geometry of the  
82 specimens, the type of mortar, or the thickness of mortar joints) was discussed  
83 in terms of dimensionless groups. Then, a dataset gathered from the existing  
84 literature was collected and discussed considering these dimensionless groups.  
85 Subsequently, the dataset was clustered in order to obtain subsets with homo-  
86 geneous values of the dimensionless groups and was used for a new calibration  
87 of the power model. Finally, the quality of the new best-fitted parameters was  
88 discussed considering their confidence intervals and three regression estimators.

Model	$K$	$\alpha$	$\beta$	$R^2$
Eurocode 6 [17]	0.55	0.70	0.30	–
Hendry and Malek [19]	1.29	0.52	0.19	
Lumantarna et al. [20]	0.75	0.75	0.31	0.87
Mann [21]	0.83	0.67	0.18	–
Kaushik et al. [22]	0.63	0.49	0.32	0.93
Gumaste et al. [23]	0.23	0.85	0.15	–
Dayaratnam [24]	0.28	0.50	0.50	–

**Table 1:** Power model  $f_M = K f_b^\alpha f_m^\beta$  for masonry compressive strength: coefficients proposed by some authors and corresponding coefficient of determination  $R^2$ .

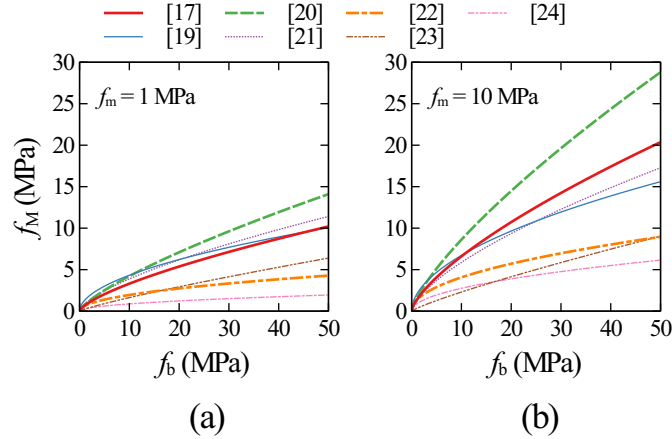


**Fig. 1:** Comparison of different power models proposed in the literature to evaluate the compressive strength of masonry  $f_M$  as a function of brick strength  $f_b$ : (a) mortar strength  $f_m = 1$  MPa; (b)  $f_m = 10$  MPa.

89 **2. Dimensional analysis**

90 *2.1. Application of Dimensional Analysis to masonry compressive strength*

91 Dimensional Analysis provides useful information when it is necessary to  
 92 identify phenomenological equations whose structure is unknown [25–27]. The  
 93 key stone of Dimensional Analysis is the Buckingham  $\Pi$  theorem, which states  
 94 that given a functional relationship  $g(\cdot)$  between  $m$  dimensional variables (with  
 95 physical dimensions)  $q_1, q_2, \dots, q_m$

$$q_1 = g(q_2, q_2, \dots, q_m) \quad (2)$$

96 then it is possible to express the process as a function of  $n = m - r$  dimensionless  
 97 parameters  $(\Pi_1, \Pi_2, \dots, \Pi_{m-r})$  as

$$\Pi_1 = \tilde{g}(\Pi_2, \Pi_3, \dots, \Pi_{m-r}) \quad (3)$$

98 where  $r$  is the number of  $m$  variables which are dimensionally independent  
 99 (equivalent to the rank of the dimensional matrix).

100 To apply Buckingham theorem to the case of masonry compressive strength  
 101  $f_M$ , we start by expressing  $f_M$  as a function of all the parameters that have  
 102 been recognized in the literature as the main factors governing the problem (a  
 103 clear description is reported for instance in [28] and [29]):

$$f_M = g(\underbrace{f_b, f_{tb}, E_b, f_m, f_{tm}, E_m, \nu_b, \nu_m, f_{fb}, f_{vb}}_{\text{mechanical properties}}, \underbrace{h_b, b_b, t_b, h_M, b_M, t_M, h_m}_{\text{geometric properties}}, c_{sh}, \dot{\sigma}, \dot{\epsilon}), \quad (4)$$

104 where  $f_b, f_{t,b}, E_b$  are compressive strength, tensile strength and Young modulus  
 105 of bricks,  $f_m, f_{t,m}, E_m$  are compressive strength, tensile strength, and Young  
 106 modulus of mortar,  $\nu_b, \nu_m$  are Poisson coefficients of bricks and mortar respec-  
 107 tively,  $f_{fb}$  and  $f_{vb}$  are the brick-mortar flexural and shear bond strengths re-  
 108 spectively,  $h_b, b_b, t_b$  and  $h_M, b_M, t_M$  are height, length, and thickness of bricks  
 109 and masonry specimens respectively,  $h_m$  is the height of mortar joints,  $c_{sh}$  is  
 110 a shape factor which takes into account the type of brickwork bond,  $\dot{\sigma}$  is the

111 loading rate, and  $\dot{\epsilon}$  is a strain rate similar to the one adopted in [30]. Eq. (4) de-  
 112 scribes the problem with  $m = 18$  dimensional variables and three dimensionless  
 113 parameters.

114 The mechanical problem can be defined in terms of three fundamental vari-  
 115 ables, e.g. mass  $M$ , length  $L$ , and time  $T$ . The corresponding dimensional  
 116 matrix (of the dimensional variables) is:

	$f_M$	$f_b$	$f_{tb}$	$E_b$	$f_m$	$f_{tm}$	$E_m$	$f_{fb}$	$f_{vb}$	$h_b$	$b_b$	$t_b$	$h_M$	$b_M$	$t_M$	$h_m$	$\dot{\sigma}$	$\dot{\epsilon}$
$M$	1	1	1	1	1	1	1	1	1	0	0	0	0	0	0	0	1	0
$L$	-1	-1	-1	-1	-1	-1	-1	-1	-1	1	1	1	1	1	1	1	-1	0
$T$	-2	-2	-2	-2	-2	-2	-2	-2	-2	0	0	0	0	0	0	0	-3	-1

(5)

117 The rank of the matrix is  $r = 3$ , therefore, according to the Buckingham  
 118 theorem, the (maximum) number of dimensionless groups that rule the prob-  
 119 lem is  $n = m - r = 15$ . Following the Buckingham's theorem, the dimen-  
 120 sionless strength  $\Pi_1$  can be expressed as a function of 14 dimensionless groups  
 121 ( $\Pi_2, \dots, \Pi_{15}$ ) and 3 dimensionless parameters ( $\nu_b, \nu_m, c_{sh}$ ) as:

$$\Pi_1 = \tilde{g}(\Pi_2, \Pi_3, \dots, \Pi_{15}, \nu_b, \nu_m, c_{sh}). \quad (6)$$

122 Buckingham's theorem provides the number of independent dimensionless  
 123 groups  $\Pi$  but their form remains unknown. Furthermore, the choice of  $\Pi$  groups  
 124 is not unique and identifying the most meaningful for a specific problem is not  
 125 a trivial task.

## 126 2.2. Choice of the dimensionless groups

127 To define the dimensionless groups it is convenient to refer to groups usu-  
 128 ally recognized as important, bearing a physical meaning, in the literature on  
 129 masonry. A possible expression is:

$$\frac{f_M}{f_b} = \tilde{g} \left( \frac{f_{tb}}{f_b}, \frac{E_b}{f_b}, \frac{f_m}{f_b}, \frac{f_{tm}}{f_b}, \frac{E_m}{f_b}, \frac{f_{fb}}{f_b}, \frac{f_{vb}}{f_b}, \frac{b_b}{h_b}, \frac{t_b}{h_b}, \frac{h_M}{h_b}, \frac{b_M}{h_b}, \frac{t_M}{h_b}, \frac{h_m}{h_b}, \frac{\dot{\sigma}}{\dot{\epsilon} f_b}, \nu_b, \nu_m, c_{sh} \right) \quad (7)$$

130 which is one of the simplest, but other groups are possible. For instance, the  
 131 group  $h_M/h_b$  could be replaced with the group  $(h_M/t_M) \times (t_M/t_b) \times (t_b/h_b)$   
 132 where the ratio  $(h_M/t_M)$  is called slenderness of the specimen and  $(t_M/t_b)$  is  
 133 the number of wythes. Besides, in [28] the shape factor  $c_{sh}$  is replaced with  
 134 the volume fraction of bricks  $VF_b$  (i.e., the ratio between volume of bricks and  
 135 that of the specimen) and the volume fraction of mortar  $VR_{mH}$  (i.e., the ratio  
 136 between volume of mortar in horizontal joints and total volume of mortar); both  
 137 could be here considered as alternative dimensionless groups. Furthermore, if  
 138 mortar is not applied uniformly, it is necessary to introduce the ratio of the  
 139 bed-joint area to the gross area.

140 It is important to notice that not all the groups have the same relevance,  
 141 and some choices could be better than others.

### 142 2.3. Reducing the number of dimensionless groups

143 It is still difficult to calibrate a phenomenological equation with all this  
 144 dimensionless groups, because the number of variables is high. In general, it  
 145 would be convenient to reduce the number of variables and consequently the  
 146 enormous number of tests that need to be performed to calibrate the equation.

147 This is possible, for instance, considering that the tensile strength  $f_{tb}$  and  
 148 the Young modulus  $E_b$  of the bricks are dependent variables since they can  
 149 be written as a function of the compressive strength  $f_b$  by means of empirical  
 150 equations like  $f_{tb} = c_1 f_b^{c_2}$  and  $E_b = c_3 f_b^{c_4}$ , where  $c_1, c_2, c_3, c_4$  are suitable coef-  
 151 ficients [31]. In this case, the variables  $f_{t,b}/f_b$  and  $E_b/f_b$  can be removed from  
 152 Eq. (7) introducing an uncertainty related to the adopted empirical equations.  
 153 The same simplification can be done for the mortar, so obtaining

$$\frac{f_M}{f_b} = \tilde{g} \left( \frac{f_m}{f_b}, \frac{f_{fb}}{f_b}, \frac{f_{vb}}{f_b}, \frac{b_b}{h_b}, \frac{t_b}{h_b}, \frac{h_M}{h_b}, \frac{b_M}{h_b}, \frac{t_M}{h_b}, \frac{h_m}{h_b}, \frac{\dot{\sigma}}{\dot{\epsilon} f_b}, \nu_b, \nu_m, c_{sh} \right) \quad (8)$$

154 and reducing to  $m = 11$  the number of dimensionless variables, plus three  
 155 parameters. However, we notice that the coefficients  $c_i$  of the adopted empirical  
 156 expressions change with the type of brick and mortar, and therefore Eq. (8)

157 should refer in principle to a specific type of brick (e.g. extruded clay, pressed  
 158 clay, calcium silicate, concrete, etc.) and mortar (e.g. cement, cement-lime, or  
 159 lime). In other words, while Eq. 7 is quite general allowing a unified approach  
 160 to the problem, Eq. 8 is specific, at least in principle, for a certain type of units  
 161 and binder because it does not explicitly consider their different mechanical  
 162 properties.

163 Further simplifications derive from the evidence that, in many tests, some  
 164 variables assume a constant value. To the purpose, Sonin [32] demonstrated  
 165 that, given a functional relationship between  $m$  quantities, of which  $r$  are di-  
 166 mensionally independent, if  $m_k$  quantities assume constant value in all the cases  
 167 being considered, then it is possible to express the process as a function of  
 168  $n = m - r - (m_k - r_k)$  dimensionless groups, where  $r_k$  is the number of  $m_k$   
 169 variables which are independent (equivalent to the rank of the dimensional ma-  
 170 trix) [32]. In passing, this is not equivalent to eliminate the role of the constant  
 171 dimensionless groups in describing the process, but simply gives the possibility  
 172 to neglect those constant groups in the interpretation of the experiments.

173 Following Sonin's theorem, one might perform the tests by using bricks of  
 174 standard (constant) dimensions. In this case,  $h_b$ ,  $b_b$ , and  $t_b$  are constant and  
 175 their corresponding dimensional matrix (in terms of dimensional variables)

$$\begin{array}{c|ccc}
 & h_b & b_b & t_b \\
 \hline
 M & 0 & 0 & 0 \\
 L & 1 & 1 & 1 \\
 T & 0 & 0 & 0
 \end{array} \tag{9}$$

176 involves  $m_k = 3$  variables whereas the rank of this matrix is  $r_k = 2$ . The  
 177 dimensional matrix in Eq. 9 is a sub-matrix of the one in Eq. 5. Applying Sonin's  
 178 theorem, the number of dimensionless groups becomes  $n = m - r - (m_k - r_k) = 9$ .  
 179 In other words, performing the tests by using standard-size bricks would simplify  
 180 data interpretation permitting, for instance, to remove the dimensionless groups  
 181  $b_b/h_b$  and  $t_b/h_b$  from Eq. (8), obtaining:

$$\frac{f_M}{f_b} = \tilde{g} \left( \frac{f_m}{f_b}, \frac{f_{fb}}{f_b}, \frac{f_{vb}}{f_b}, \frac{h_M}{h_b}, \frac{b_M}{h_b}, \frac{t_M}{h_b}, \frac{h_m}{h_b}, \frac{\dot{\sigma}}{\dot{\epsilon} f_b}, \nu_b, \nu_m, c_{sh} \right) \quad (10)$$

182 Of course, this simplification absolutely does not mean that the size of the  
 183 bricks is physically irrelevant; it is just an experimental assumption that permits  
 184 to focus on the effect of the other dimensionless parameters.

#### 185 2.4. Dimensional analysis and power equation

186 Dimensional Analysis does not provide information on the analytical expres-  
 187 sion for the equation  $\tilde{g}(\cdot)$  governing the problem.

188 The analytical expression of  $\tilde{g}(\cdot)$  can be chosen to be particularly suitable  
 189 for data fitting and regression algorithms. This is the case of the equation:

$$\frac{f_M}{f_b} = k \left( \frac{f_m}{f_b} \right)^{\beta_1} \times \left( \frac{f_{fb}}{f_b} \right)^{\beta_2} \times \left( \frac{f_{vb}}{f_b} \right)^{\beta_3} \times \left( \frac{b_b}{h_b} \right)^{\beta_4} \times \left( \frac{t_b}{h_b} \right)^{\beta_5} \times \dots \quad (11)$$

190 where  $k, \beta_1, \beta_2, \dots$  are coefficients. The equation is obtained by multiplying  
 191 the powers of all the dimensionless groups in Eq. (8). If only the dimensionless  
 192 group  $f_m/f_b$  varies whereas all the other remain constant, Eq. (11) becomes:

$$\frac{f_M}{f_b} = K \left( \frac{f_m}{f_b} \right)^{\beta} \quad (12)$$

193 OR

$$f_M = K f_b^{1-\beta} f_m^{\beta} = K f_b^{\alpha} f_m^{\beta} \quad (13)$$

194 with  $\alpha = 1 - \beta$ , which is the well-known power equation usually adopted in the  
 195 literature for masonry compressive strength (Eq. 1).

196 Equation (13), like Eq. (8), is specific for a given type of unit and binder  
 197 because it does not explicitly consider their different mechanical properties. It  
 198 is evident from Eq. (12) that, if just one of the constant dimensionless groups  
 199 not explicitly considered in Eq. (13) varies, the coefficients of the equation will  
 200 be different. This clearly explains the important differences between dimension-  
 201 less coefficient  $K$  of the power equations proposed in the literature (Tab. 1).  
 202 The variations of the exponents  $\alpha$  and  $\beta$  can be explained considering that

203 Eq. (12) is oversimplified; for instance also the powers  $\beta_i$  could be functions of  
204 the dimensionless parameters.

205 From a mechanical viewpoint, these differences can be explained considering  
206 that masonry specimens display different failure modes depending both on the  
207 properties of brick and mortar and on the loss of bond between them [33]. In [23]  
208 four different failure modes were observed: in case of bricks stiffer than mortar,  
209 a triaxial compression occurs in the mortar whereas bricks are subjected to com-  
210 pression/biaxial tension up to possible debonding between the two materials.  
211 In case of mortar stiffer than bricks, instead, the triaxial compression occurs in  
212 the bricks whereas mortar is subjected to compression/biaxial tension. Assum-  
213 ing that there is a relationship between stiffness of the components and their  
214 compressive strength, it is possible to suppose that the behavior is ruled by the  
215 ratio  $f_m/f_b$ . This scenario is modified by the presence of vertical mortar joints  
216 (considered by coefficient  $c_{sh}$ ) and by loss of bond between bricks and mortar  
217 (accounted by  $f_{vb}/f_b$  and  $f_{fb}/f_b$ ). The structure of Eq. (13) is too simple to  
218 catch all failure modes and distinct procedures of calibration and coefficients are  
219 necessary, at least for the two cases of bricks stronger and weaker than mortar  
220 (i.e.  $f_m/f_b > 1$ ).

221 The use of the Dimensional Analysis has proven some theoretical limits of  
222 the power equation and has explained the variability of its coefficients. In the  
223 next section these aspects will be considered for a proper calibration of a new  
224 power equation.

### 225 **3. Experimental dataset**

#### 226 *3.1. Description of the dataset*

227 In order to discuss the power equation, it was necessary to collect a database  
228 of experimental data that comprehends all the dimensionless variables grouped  
229 in Eq. (8). Because the equation is specific to a given type of brick and mor-  
230 tar, it was necessary to limit the attention to a certain type of masonry. For  
231 the reasons explained in the introduction, the database has been prepared by

	$f_M$	$f_b$	$f_m$	$b_b$	$t_b$	$h_b$	$h_M$	$t_M$	$h_m$
	(MPa)	(MPa)	(MPa)	(mm)	(mm)	(mm)	(mm)	(mm)	(mm)
min	0.74	6.81	0.60	200.0	100.0	50.0	300.0	100.0	8.00
mean	7.84	17.68	5.74	239.4	115.3	59.7	441.8	151.2	10.55
max	14.98	32.00	13.85	280.0	140.0	75.5	800.0	260.0	15.00

**Table 2:** Variations of the parameters of the analyzed dataset for wallettes.

232 searching the literature for compression tests on specimens made of solid-clay-  
233 bricks. Of course, the approach that will be followed, being completely general,  
234 is also valid for other types of masonry, such as concrete block masonry. Only  
235 wallettes and stack-bonded prisms specimens were considered because they re-  
236 ceived more attention in the literature. To collect the data, the database MADA  
237 [34] has also been used. Unfortunately, many studies with interesting experi-  
238 mental campaigns have been discarded because they contained incomplete data.  
239 Specimens with bricks weaker than mortar have been discarded too, since they  
240 display a different failure mode with respect to the one with bricks stronger than  
241 mortar [35], which are the majority of experimental data. Finally, a set of 116  
242 values from 24 references has been collected [6, 18, 20, 23, 36–55]. The data are  
243 reported in Tabs. A1 and A2 of the Appendix, for wallettes and stack-bonded  
244 prism specimens respectively. The tables include the strengths of masonry  $f_M$ ,  
245 bricks  $f_b$ , and mortar  $f_m$ , the dimensions of both walls ( $b_M \times h_M \times t_M$ ) and  
246 bricks ( $b_b \times h_b \times t_b$ ), and the thickness of mortar joints  $h_m$ . In addition, avail-  
247 able information on number of wythes, and mortar type (cement  $c$ , cement-lime  
248  $c + l$ , and lime  $l$ ) have been indicated. Bond strengths  $f_{fb}$  and  $f_{vb}$  were not  
249 reported because of the scant or null information in the considered experimental  
250 campaigns.

251 Wallettes and stack-bonded prisms display a different behavior [56], there-  
252 fore they have been studied separately taking into account implicitly the shape  
253 parameter  $c_{sh}$ . According to EC6 [17], tests on wallettes are performed follow-  
254 ing EN1052-1 [57] code, which prescribes standard values for the load speed.  
255 For this reason, the dimensionless parameter  $\dot{\sigma}/\dot{\epsilon}f_b$  can be considered constant.

	$f_M$ (MPa)	$f_b$ (MPa)	$f_m$ (MPa)	$b_b$ (mm)	$t_b$ (mm)	$h_b$ (mm)	$h_M$ (mm)	$t_M$ (mm)	$h_m$ (mm)
min	2.90	7.50	0.69	191.0	89.0	50.0	250.0	89.0	7.50
mean	13.33	29.22	9.33	229.6	109.2	62.3	313.8	109.7	12.13
max	37.70	68.73	52.60	290.0	140.0	78.0	523.0	140.0	15.00

**Table 3:** Variations of the parameters of the analyzed dataset for stack-bonded prisms.

	$f_M/f_b$ (-)	$f_m/f_b$ (-)	$b_b/h_b$ (-)	$t_b/h_b$ (-)	$h_M/h_b$ (-)	$h_M/t_M$ (-)	$t_M/h_b$ (-)	$h_m/h_b$ (-)
min	0.06	0.05	2.86	1.43	5.45	2.14	1.52	0.14
mean	0.45	0.33	4.11	1.99	7.63	3.11	2.69	0.17
max	0.86	0.83	5.09	2.55	11.80	4.17	5.20	0.21

**Table 4:** Variations of the dimensionless parameters of the analyzed dataset for wallettes.

	$f_M/f_b$ (-)	$f_m/f_b$ (-)	$b_b/h_b$ (-)	$t_b/h_b$ (-)	$h_M/h_b$ (-)	$h_M/t_M$ (-)	$t_M/h_b$ (-)	$h_m/h_b$ (-)
min	0.20	0.05	2.92	1.44	3.21	1.89	1.44	0.13
mean	0.53	0.35	3.84	1.82	5.20	2.92	1.83	0.20
max	1.08	1.00	5.80	2.80	8.77	5.51	2.80	0.30

**Table 5:** Variations of the dimensionless parameters of the analyzed dataset for stack-bonded prisms.

256 The same applies for stack-bonded prisms, which are usually tested according  
257 to ASTM 1314-18 [58]. Tables 2 and 3 show the minimum, mean, and max-  
258 imum values of the parameters of wallettes and stack-bonded prisms datasets  
259 respectively. For the same datasets, Tables 4 and 5 represents the minimum,  
260 mean, and maximum values of the considered dimensionless parameters, already  
261 defined in Eq. (8). Tabs. 2, 4 show that wallettes substantially fulfill the me-  
262 chanical and geometrical limits prescribed by EC6 [17] and EN1052-1 [57]. Also  
263 for stack-bonded prisms, Tabs. 3 and 5 show that the prescription of ASTM  
264 1314-18 [58] are mostly satisfied.

265 The number of samples (41 and 75 for wallettes and stack-bonded prisms  
266 respectively), although limited, is sufficient to perform some statistical stud-  
267 ies. However, since data have been measured sometimes with heterogeneous  
268 specimens and testing conditions, data preparation and discussion by means of  
269 Dimensional Analysis will be performed before proceeding with their study.

### 270 3.2. Correction of brick and mortar strengths

271 The power model employs the mean compressive strengths of bricks and  
272 mortar as input variables. For the considered dataset, these values have been  
273 measured following different standard codes, humidity conditions, and geome-  
274 try of the specimens. Regarding the geometry, it is known that size and shape  
275 of brick specimens influence their failure mode and, consequently, the mea-  
276 sured strength [59]. For this reason, EC6 [17] employs in the power equation  
277 the normalized strength  $f'_b = \delta f_b$ , where the coefficient  $\delta$ , defined in EN772-1  
278 [60], transforms the measured strength to the one of a reference cube of side  
279 100 mm. The same correction coefficient  $\delta$  was used in [61, 62] to homogenize  
280 their database of hollow concrete blocks. Since this correction seems to be ac-  
281 cepted by the scientific community, it was used in the present work to compute  
282 the normalized brick strengths  $f'_b$  reported in Tabs. A1,A2.

283 Apart these tables, in the forthcoming sections the corrected brick strength  
284  $f'_b$  will always be used although, for simplicity, it will be indicated as  $f_b$ .

285 Also the size and the slenderness of mortar samples have a recognized in-  
286 fluence on the measured value of compressive strength  $f_m$  [63]. Unfortunately,  
287 many authors do not report the adopted standards, nor the size of the mortar  
288 specimens; therefore it was not possible to correct the values of  $f_m$ .

### 289 3.3. Correction for masonry slenderness

290 The slenderness of the specimens (i.e. the ratio of the height to the least  
291 lateral dimension of the prism  $h_M/t_M$ ) plays an important role in masonry com-  
292 pressive strength [64–68]. The slenderness  $h_M/t_b$  should be chosen to correctly  
293 represent the behavior of real walls subjected to pure compression. For this  
294 reason, the slenderness should be limited to reduce the eccentricity due to con-  
295 struction imperfections and second order effects [68]. Furthermore, squat speci-  
296 mens are easier to build or extract from existing masonry and for this reason are  
297 allowed by different standard codes. In this case, a minimum of three courses  
298 of bricks ( $h_M/h_b \geq 3$ ) is indispensable to prevent the effect of end restraints -  
299 exerted by the platens of the testing machine on the lateral deformation of the  
300 specimen - from altering the masonry failure mode [69]. As observed in [65], it  
301 seems that only for a slenderness  $h_M/t_M > 6$ , the effect of end restrains vanishes  
302 and pure compressive strength is attained. The restraints can be reduced by  
303 introducing a layer of suitable frictionless material between the specimen and  
304 the load bearing platens of the testing machine. Of course, different friction-  
305 less materials produce different effects on the measured strength [46, 55]. For  
306 this reason, some standard codes, rather than adopting frictionless interlayers,  
307 prefer to recommend a specific slenderness. For instance, Fig. 2 shows the sizes  
308 required by EN1052-1 [57] (for units with  $h_b \leq 150$  mm and  $b_b \leq 300$  mm)  
309 and ASTM 1314-18 [58] standard codes. Furthermore, the ASTM 1314-18 [58]  
310 adopts correction factors to transform the measured strength to the one of a  
311 reference specimen with slenderness  $h_M/t_M = 2$ . On the contrary, UNI 1052-1  
312 [57] prescribes specimens with  $h_M/t_M > 3$ , without any correction factor.

313 The choice of a well-suited correction function is not trivial. The high num-  
314 ber of solutions proposed in the literature as well as in standard codes reveals

315 that the problem is still open [70]. For instance, in [61, 62] the ASTM 1314-  
 316 18 correction function was used for concrete masonry prisms. In [28], instead,  
 317 it was preferred to calibrate the correction function together with the power  
 equation.

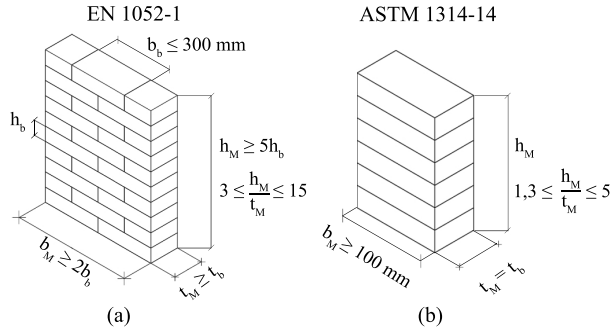


**Fig. 2:** Shape of masonry prisms recommended by Standard Codes: (a) EN1052-1 [57]; (b) ASTM 1314-18 [58].

318

319 In the present work, wallettes fulfill the geometric limits prescribed by EN1052-  
 320 1 therefore, according to the same code, no correction function was introduced.  
 321 On the contrary, test on stack-bonded prisms were performed according to  
 322 ASTM 1314-18 and the correction function prescribed by the same code, which  
 323 seems to be well accepted by the scientific community, was applied. The cor-  
 324 rected compressive strengths  $f'_M$  thus obtained are reported in Tab. A2. Apart  
 325 this table, in the forthcoming sections the corrected masonry strength  $f'_M$  will  
 326 always be used for stack-bonded prisms but, for homogeneity with wallettes, it  
 327 will be indicated as  $f_M$ .

### 328 3.4. Discussion of the dataset considering the dimensionless parameters

329 The corrected dataset is now discussed starting from wallettes. Fig. 3 shows  
 330 the masonry dimensionless strength  $f_M/f_b$  as a function of mortar dimension-  
 331 less strength  $f_m/f_b$ . In Fig. 3a the data are represented distinguishing the  
 332 number of wythes ( $t_M/t_b$ ). The figure clearly shows that two-wythes wallettes  
 333 present smaller strengths with respect to one-wythe, as already highlighted by

334 some authors [17, 19]. For this reason one-wythe and two-wythe data must  
 335 be studied separately. In the collected dataset, one-wythe wallettes are the  
 336 majority therefore the subsequent figures are specific for one-wythe masonry  
 337 ( $t_M/t_b = 1$ ). In Fig. 3b the data are represented considering the type of mortar  
 338 (cement, cement-lime, and lime): differences between the three types are not  
 339 so evident but deserve to be investigated. Fig. 3c represents the effect of the  
 340 dimensionless parameter  $h_M/h_b$ , related to the number of courses, which is not  
 341 self-evident. The same can be said for the slenderness  $h_M/t_M$  considered in  
 342 Fig. 3d. This seems to justify, for the considered dataset, the choice of having  
 343 omitted a correction factor for the slenderness. The effect of the thickness of  
 344 mortar joints is represented in Fig. 3e by means of the dimensionless parameter  
 345  $h_m/h_b$ . Also in this case, data do not show different trends for the different val-  
 346 ues of  $h_m/h_b$ . Finally, Figs. 3f,g represent the effect of brick geometry by means  
 347 of the dimensionless parameters  $t_b/h_b$  and  $b_b/h_b$ . Data display an homogeneous  
 348 behavior; therefore the dimensionless sizes of the bricks can be considered to  
 349 be constant, as in the previous example on Sonin's theorem. Based on this  
 350 analysis, it seems correct to perform the best fitting of the dataset of wallettes  
 351 by distinguishing the number of wythes and the type of mortar, whereas all the  
 352 other dimensionless groups will be considered to be constant.

353 Considering stack-bonded prisms, Fig. 4a shows the importance of mortar  
 354 type: imagining an ideal bisector line from the lower left to the upper right  
 355 corners of the figure, points corresponding to lime mortar are clustered in the  
 356 upper part with respect to this line. The effect of dimensionless parameter  
 357  $h_M/h_b$  can be observed in Fig. 4b. The most surprising aspect is that speci-  
 358 mens with  $6 < h_M/h_b \leq 8$  are clustered in the lower part of the plot whereas  
 359 specimens with  $2 < h_M/h_b \leq 4$  are grouped at the top. This effect is more  
 360 evident in Fig. 4c where the slenderness  $h_M/t_M$  is considered: squat specimens  
 361 are placed in the upper part of the plot whereas slender specimens are placed  
 362 in the bottom part. The effect is evident also in case of uncorrected masonry  
 363 strengths  $f_M$  (Figs. 4d). Interestingly, it seems that the adopted ASTM1314-18  
 364 correction function is not able to remove completely the effect of slenderness for

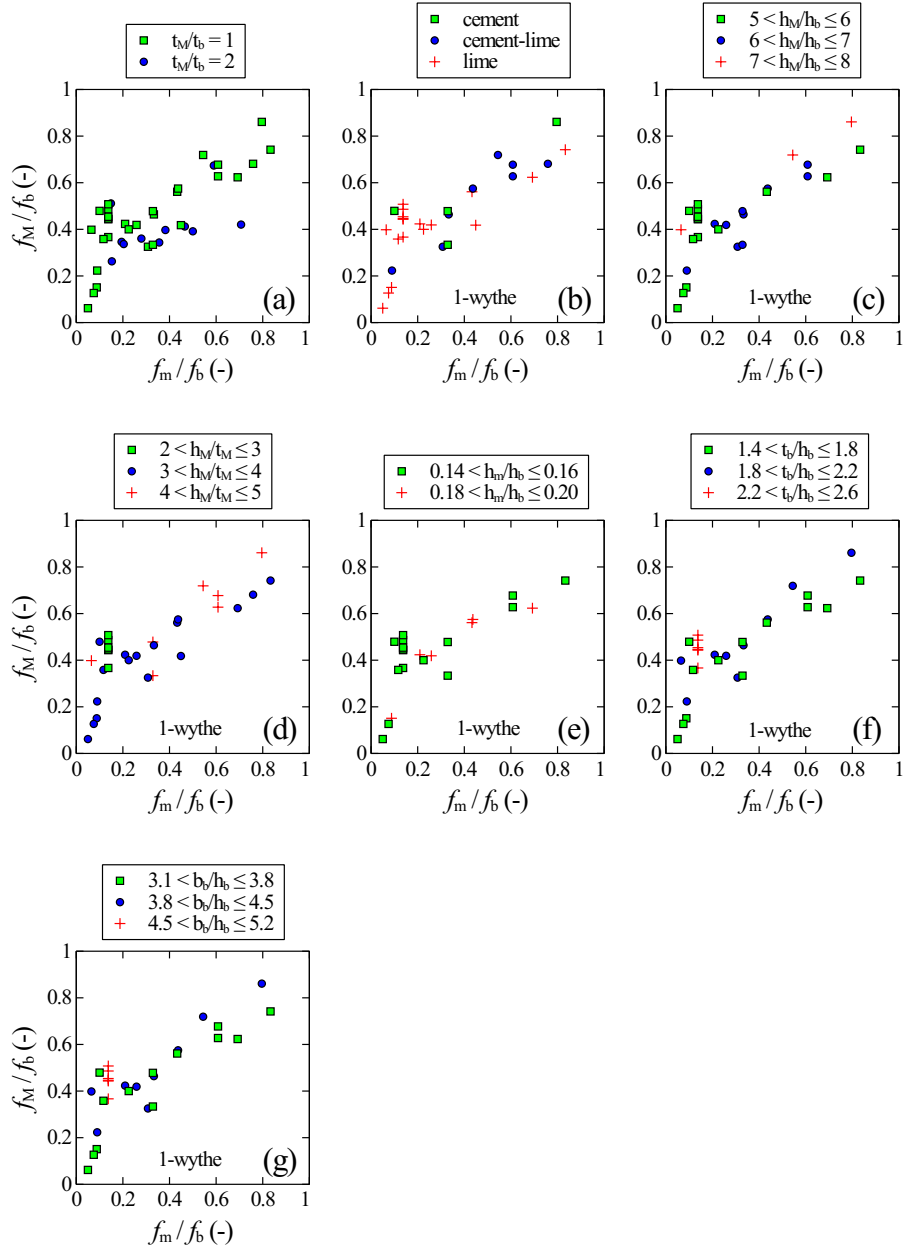


**Fig. 3:** Wallettes: (a) effect of the number of wythes  $t_M/t_b$ ; (b) effect of mortar type; (c) effect of  $h_M/h_b$ ; (d) effect of  $h_M/t_M$ ; (e) effect of mortar joint thickness  $h_m/h_b$ ; (f) effect of brick size  $t_b/h_b$ ; (g) effect of brick size  $b_b/h_b$ .

365 the considered dataset. This problem has already been raised in [71] for concrete  
 366 masonry prisms. Fig. 4e shows the effect of mortar thickness  $h_m/h_b$ . As in the  
 367 case of wallettes, data do not display a specific trend. The same can be said  
 368 for the brick dimensions  $t_b/h_b$  and  $b_b/h_b$  shown in Figs. 4f,g. According to this  
 369 graphic analysis, it seems possible to perform the best fitting of the dataset of  
 370 stack-bonded prisms by distinguishing the type of mortar and the slenderness  
 371 of the specimens  $h_M/t_M$ , which seems to be the most meaningful dimensionless  
 372 groups, whereas all the others will be considered to be constant.

#### 373 4. Calibration of a new power equation

374 The obtained results suggest trying a new calibration of the power model –  
 375 which is specific for solid clay bricks – by distinguishing the different dimension-  
 376 less groups that have been recognized to be important for the collected dataset.

377 Generally, the coefficients of the power models proposed in the literature  
 378 are calibrated by minimizing the sum-of-squares ( $SS$ ) of the residuals  $X =$   
 379  $f_{M,test} - f_{M,model}$ , defined as “vertical” distance between experimental points  
 380 and surface, by means of the Minimum Least Square Method (MLSM). This  
 381 method is based on the hypothesis that the residuals  $X$  follow a Gaussian dis-  
 382 tribution with constant variance (homoscedasticity). In addition, the method  
 383 requires that independent variables are measured with much greater precision  
 384 than the dependent ones. These hypotheses, which are usually taken for granted,  
 385 are now verified before proceeding with the calibration of the model.

386 Here, the power equation

$$f_M = K f_b^\alpha f_m^{1-\alpha} \quad (14)$$

387 was used, where  $K$  and  $\alpha$  are the parameters to be fitted. Equation (14) was  
 388 preferred to Eq. (1) because it is more consistent from the point of view of di-  
 389 mensional analysis, since the coefficient  $K$  is dimensionless and does not change  
 390 with the adopted units. Furthermore, Eq. (12) was not used because, when di-  
 391 viding  $f_M$  by  $f_b$ , the nonlinear transformation modifies also the distribution of

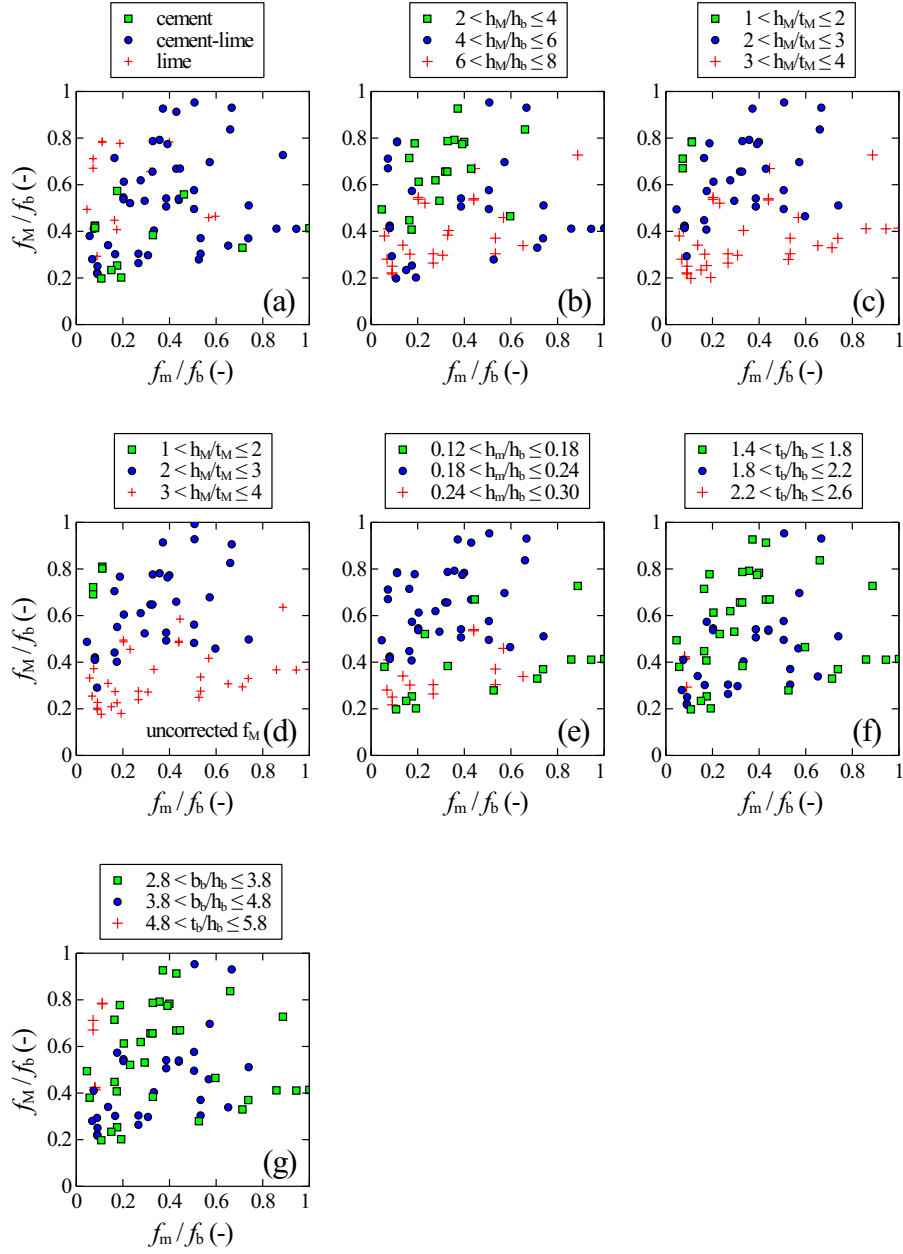


**Fig. 4:** Stack-bonded prisms: (a) effect of mortar type; (b) effect of  $h_M/h_b$ ; (c) effect of slenderness  $h_M/t_M$ ; (d) effect of slenderness  $h_M/t_M$  for uncorrected strengths  $f_M$ ; (e) effect of mortar joint thickness  $h_m/h_b$ ; (f) effect of brick size  $t_b/h_b$ ; (g) effect of brick size  $b_b/h_b$ .

392 the residuals  $|X|$ , which, as we will see, has a certain importance for the study  
393 of the regression.

394 The employed equation requires to solve a problem of nonlinear regression  
395 with unknowns  $K$  and  $\alpha$ . Transformation of Eq. (14) by means of logarithms  
396 would simplify the problem to a linear regression

$$\ln f_M = \ln K + \alpha \ln f_b + (1 - \alpha) \ln f_m \quad (15)$$

397 with unknowns  $\ln K$  and  $\alpha$ . However, this transformation would also modify the  
398 distribution of the residuals  $X$ , and therefore it was not applied at this stage,  
399 where it was preferred to solve the nonlinear problem by using the Matlab  
400 function `fit` [72].

401 The fitting was initially performed considering 1-wythe wallettes. The best-  
402 fitting function is represented in Fig. 5a as a surface, together with the data  
403 points. The dispersion of the points is evident; however the analysis of the data  
404 by means of matlab FSDATool [73] reveals that this dispersion is not due to  
405 outliers, therefore robust statistics was not applied.

406 The values of the fitted parameters  $K$  and  $\alpha$ , and their 95% confidence  
407 intervals, computed by means of the asymptotic method [72], are reported in  
408 Tab. 6 (wallettes 1-wythe). The 95% confidence interval has a 95% chance of  
409 containing the true value of the parameter. The corresponding upper and lower  
410 bound surfaces, plotted in Fig. 5a, show the uncertainty of the model.

411 The analysis of the residuals  $X$  permits to check if the adopted procedure  
412 fulfills the hypotheses of the MLSM. Fig. 5b shows the plot of the residuals  $X$ ,  
413 together with their best fitting plane of equation  $X = p_0 + p_1 f_b + p_2 f_m$ . Small  
414 values of the coefficients  $p_0$ ,  $p_1$ , and  $p_2$  confirm that the errors  $X$  are equally  
415 distributed above and below the plane  $X = 0$ . Fig. 5c displays the absolute  
416 value of the error  $|X|$  and the corresponding best-fitting plane. It is possible to  
417 observe that the errors, as expected, increase with  $f_b$  but the coefficients of the  
418 best fitting plane are small also in this case, therefore the hypothesis of constant  
419 variance (homoscedasticity) is not badly violated.

420 To check the hypothesis of normal distribution of the residuals  $X$ , their

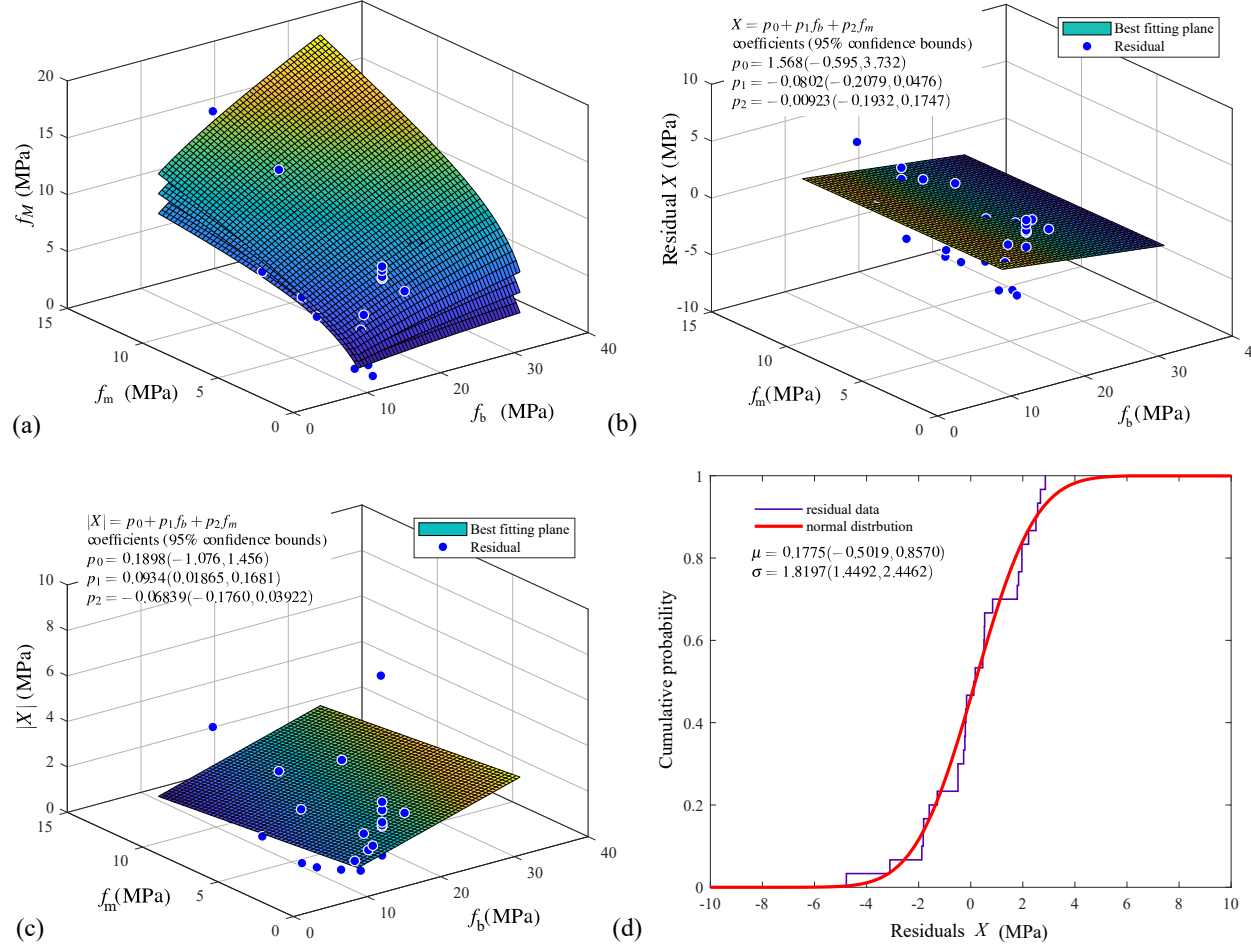


**Fig. 5:** Best fitting of all the data: (a) Comparison between best fitted model, 95% confidence bounds and experimental points; (b) Comparison between residuals  $X$  and their best-fitting plane; (c) Comparison between absolute values of the residuals  $|X|$  and their best-fitting plane; (d) Cumulative of the residuals  $X$  and fitting with normal-distribution cumulative.

421 cumulative has been plotted in Fig. 5d. The theoretical normal cumulative,  
 422 with mean  $\mu = 0.1775$  MPa and standard deviation  $\sigma = 1.8197$  MPa, is well  
 423 superimposed on the experimental curve. In addition, normality tests have  
 424 been performed. In particular, the skewness is -0.58 and Kurtosis coefficient

Type	Param.	all	cement	cement-lime	lime
Wallettes (1 wythe)	$N$	30	4	8	18
	$K$	0.79 (0.66, 0.91)	-	0.91 (0.66, 1.15)	0.70 (0.51, 0.89)
	$\alpha$	0.57 (0.44, 0.70)	-	0.33 (0.022, 0.64)	0.70 (0.54, 0.86)
Stack-bonded prisms $2 \leq h_M/t_M < 3$	$N$	35	5	22	8
	$K$	0.87 (0.74, 1.01)	-	0.76 (0.50, 1.02)	0.75 (0.28, 1.21)
	$\alpha$	0.71 (0.63, 0.80)	-	0.90 (0.55, 1.24)	0.74 (0.36, 1.11)
Stack-bonded prisms $3 \leq h_M/t_M < 4$	$N$	33	6	24	1
	$K$	0.57 (0.46, 0.68)	-	0.60 (0.47, 0.74)	-
	$\alpha$	0.75 (0.61, 0.90)	-	0.73 (0.57, 0.90)	-

**Table 6:** Parameters of the model  $f_M = K f_b^\alpha f_m^{1-\alpha}$  obtained by best fitting of  $N$  specimens, 95% confidence intervals (within parentheses).

425 is equal to 3.22. For a normal distribution, the skewness (which measures the  
426 lack of symmetry of the distribution) is zero and the Kurtosis coefficient (which  
427 measures how the data are tailed with respect to a normal distribution) is 3.  
428 With these values, it is possible to confirm the hypothesis of normal distribution  
429 of the residuals  $X$ .

430 The previous analyses of the errors show that the hypotheses of MLSM  
431 are substantially fulfilled. The only problem is that the independent variables  
432 (brick and mortar strengths) are measured with a precision comparable with  
433 the dependent ones, as suggested by their typical coefficients of variation. The  
434 problem is pointed out also in the EC6 [17], where it is specified that the pro-  
435 posed power equation is valid only for bricks whose compressive strength has a  
436 coefficient of variation smaller than 25%. To address this issue it would be nec-  
437 essary to develop new statistical tools based for instance on Total Least Squares  
438 Method [74–76], which are very complicate and out of the scope of the present  
439 work.

440 Considering the fact that all power models proposed in the literature ignored  
441 this issue obtaining satisfactory results, or at least accepted by the scientific  
442 community, MLSM was considered applicable to the problem also in the present  
443 work.

444 Therefore, fitting and validation were repeated to the sub-cases of 1-wythe  
 445 wallettes in cement-lime, and lime mortar. The case of cement was not analyzed  
 446 because of the insufficient number of experimental data ( $N = 4$ ). The values of  
 447 the determined coefficients  $K$  and  $\alpha$  are reported in Tab. 6, together with their  
 448 95% confidence intervals.

449 The importance of confidence intervals is shown in Fig. 6, where the dimen-  
 450 sionless masonry strength  $f_M/f_b$  is represented as a function of dimensionless  
 451 mortar strength  $f_m/f_b$ . In the same figure, the fitted curve is represented to-  
 452 gether with the 95% confidence band obtained using the confidence intervals  
 453 as coefficients of the power model. The confidence band shows how well we  
 454 know the curve. The dispersion of the data and their limited number implies  
 455 rather wide confidence bands. Probably the results would improve increasing  
 456 the number of data points.

457 Fitting was repeated for stack-bonded prisms distinguishing slenderness  $2 \leq$   
 458  $h_M/t_M < 3$  and  $3 \leq h_M/t_M < 4$ . Results are reported in Tab. 6 considering  
 459 all the data and, subsequently, separating the mortar type. Cases with  $N < 8$   
 460 were not analyzed because of the scant number of points.

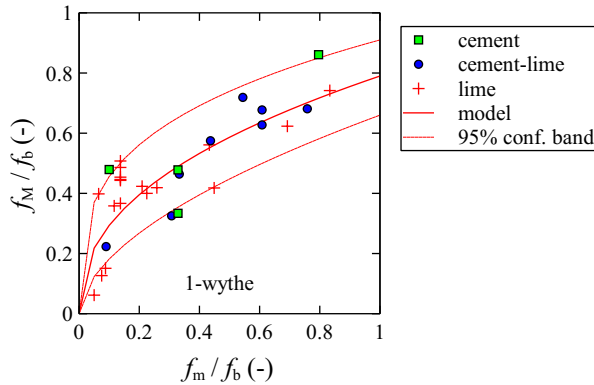


**Fig. 6:** Results of fitting of 1-wythe wallettes (all data) and corresponding confidence band.

461 Also in the case of stack-bonded prisms, coefficients reported in Tab. 6 dis-  
 462 play an important variation an wide 95% confidence limits.

463 Despite this problem, it is interesting to notice that the coefficients for stack-  
464 bonded prisms are different from the ones for wallettes. Furthermore, the dif-  
465 ferent slenderness and mortar type imply, as expected, different coefficients.

## 466 5. Discussion of the results

### 467 5.1. Wallettes

468 The quality of the proposed regressions was investigated starting from one-  
469 wythe wallettes (all data). The predicted strengths  $f_{M,model}$  are plotted in  
470 Fig. 7a as a function of the corresponding measured strengths  $f_{M,test}$ , together  
471 with the bisector line that represents the ideal perfect correspondence between  
472 the test results and the proposed model. Points above the bisector line lay on  
473 the unsafe side. In the same figure, the dashed lines represent an error of  $\pm 20\%$   
474 in the model.

475 The study is repeated in Fig. 7b for EC6 [17] model. A coefficient of 1.2 was  
476 used according to [17] to transform the characteristic strengths into the mean  
477 strengths. As can be seen, the results are similar to the ones of the proposed  
478 regression in the case of low strengths but some points lay on the unsafe side for  
479 higher strengths. Fig. 7c shows the behavior of the model proposed by Hendry  
480 & Malek [19]. In this case, most of the points lay on the safe side with important  
481 errors. The same can be said for the Mann's model [21].

482 To quantify numerically the goodness of the fit, the classic coefficient of de-  
483 termination  $R^2$  was computed. Results are reported in Tab. 7. The proposed  
484 model provides the best  $R^2$ , especially when the type of mortar is distinguished.  
485 The values are not exciting, but in any case better than those of the models  
486 chosen for comparison, especially for cement-lime and lime mortar. However, it  
487 is well known that the coefficient of determination cannot be the only indicator  
488 used to judge the quality of a model. For this reason, also the Akaike's In-  
489 formation Criterion (AIC) was introduced, since it is particularly indicated for  
490 the case of non-nested models (i.e., not dependent)[77]. Because the number of  
491 data points  $N$  is small with respect to the number of model parameters  $k$ , it was

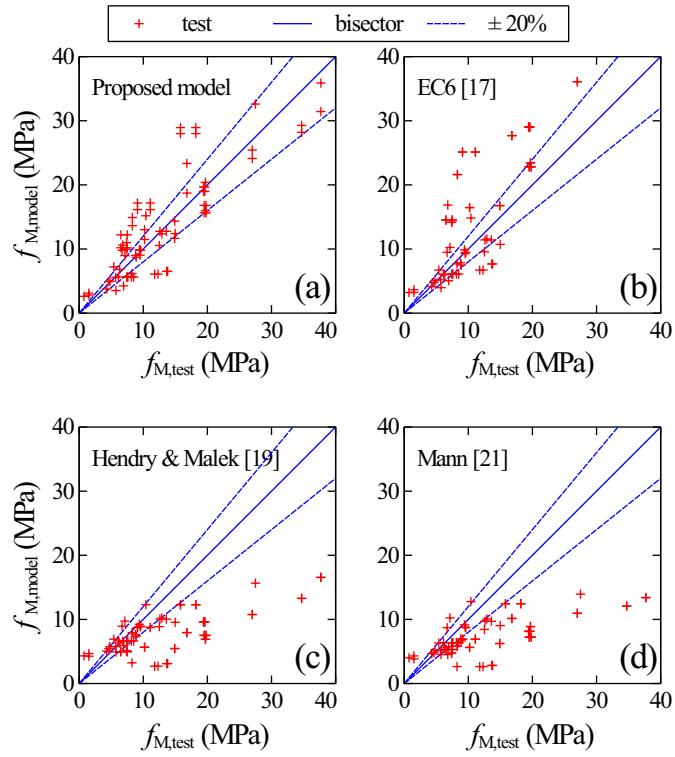


**Fig. 7:** One-wythe wallettes (all data). Comparison between experimental compressive strengths  $f_{M,test}$  and compressive strengths predicted by the calibrated model  $f_{M,model}$ : (a) Proposed model; (b) EC6 [17]; (c) Hendry & Malek [19]; (d) Mann [21].

492 preferred to use the corrected Akaike's Information Criterion ( $AIC_c$ ), defined  
493 as:

$$AIC_c = N \ln \frac{SS}{N} + 2k + \frac{2k(k+1)}{N-k-1} \quad (16)$$

494 where  $SS$  is the sum of squares of the errors  $X$ . The coefficient  $AIC_c$  can only  
495 be computed when  $N > 2k$  [77]. Comparing two models, the best one has the  
496 lowest  $AIC_c$  coefficient.

497 Also in this case, the proposed model provides better results, particularly  
498 when the type of mortar is considered (Tab. 7). It is interesting to notice that,  
499 for the proposed model and for EC6, the number of parameters is  $k = 2$  because  
500  $\alpha + \beta = 1$ . For the other two models  $k = 3$ , therefore the condition  $N > 2k$   
501 was not fulfilled in the case of cement-lime and lime mortar, and the coefficient  
502  $AIC_c$  was not computed.

503 Another indicator useful from the engineering point of view is the coefficient  
504  $a_{20}$  proposed in [14], which represents the number of points predicted with a  
505 relative error  $\leq 20\%$  with respect to the total number of points  $N$ . Comparing  
506 two models, the best one has the  $a_{20}$  coefficient closest to one.

507 If we consider all the data, the models provide similar values of  $a_{20}$ , which  
508 are close to 0.50. Instead, if the type of mortar is distinguished, the proposed  
509 model provides values of  $a_{20}$  close to 0.75, which are good and similar to those  
510 reached in [14] by means of neural networks.

511 The study suggests that also the type of mortar should be considered to  
512 define the compressive strength of solid-clay-brick wallettes.

513 Among the models proposed in the literature, the EC6 provides the best  
514 results even in the case of lime mortar. This result was not predictable because  
515 the model was proposed for general-purpose mortar. Compared to the proposed  
516 new models, although the indicators are only slightly worse, the EC6 is more  
517 conservative for higher strengths (Fig. 7).

Model	all			cement-lime			lime		
	$R^2$	$a_{20}$	$AIC_c$	$R^2$	$a_{20}$	$AIC_c$	$R^2$	$a_{20}$	$AIC_c$
Proposed	0.73	0.50	42.12	0.77	0.75	17.79	0.72	0.61	19.39
EC6 [17]	0.68	0.50	46.75	0.35	0.63	26.12	0.70	0.50	20.86
Hendry & Malek [19]	0.63	0.53	54.32	0.28	0.38	-	0.63	0.61	27.90
Mann [21]	0.57	0.47	58.42	0.08	0.25	-	0.64	0.61	27.31

**Table 7:** One-wythe wallettes: comparison of the proposed model to some models published in the literature.

518 *5.2. Stack-bonded prisms*

519 The study proposed for wallettes was repeated for stack-bonded prisms. In  
520 particular, Figs. 8, 9 show the relationship between  $f_{M,test}$  and  $f_{M,model}$  for  
521 the cases of  $2 < h_M/t_M \leq 3$  and  $3 < h_M/t_M \leq 4$  respectively. The same  
522 figures show the behavior of the models published for stack-bonded prisms by  
523 Lumantarna et al. [20], Kaushik et al. [22], and Gumaste et al. [23].

524 For the sake of completeness, comparisons with the TMS402/602-16 [78] and  
525 AS37000-18 [79] models have been included in in the same figures, even if they  
526 are not power models.

527 The points predicted by the proposed models are well distributed around  
528 the bisector line for both slendernesses (Fig. 8a, 9a). On the contrary, the  
529 model proposed by Lumantarna [20] fits well the first case with small slenderness  
530 (Fig. 8b), but provides unconservative results for the second case (Fig. 9b). This  
531 can be explained considering that Lumantarna’s model was calibrated for three-  
532 bricks-high stack-bonded prisms, which are squat and similar to the first case.  
533 The model proposed by Kaushik et al. [22], calibrated for five-bricks-high stack-  
534 bonded prisms, provides conservative results in both cases (Figs. 8c, 9c). The  
535 same can be said for the model published by Gumaste et al. [23] (Figs. 8d, 9d).

536 Figs. 8e and 9e show the results for the model proposed in TMS402/602-16  
537 [78]. The ASTM 1314-18 prism test method used for stack-bonded prisms is  
538 usually associated with the TMS402/602-16 [78] unit strength method, which  
539 provides the specified compressive strength of masonry (in psi) by means of the

540 equation:

$$f_M = A(400 + Bf_b) \quad (17)$$

541 where  $f_b$  is the average compressive strength of clay-masonry units (in psi),  
542  $A = 1$  for inspected masonry,  $B = 2$  for Type N portland-cement lime mortar,  
543 and  $B = 0.25$  for type S or M portland-cement lime mortar. The type of mortar  
544 is defined with its recipe, which is usually different from those used in the  
545 dataset. Moreover, lime mortar is not considered.

546 Since there is no direct correspondence between mortar strength and type  
547 (S, N, or M),  $B = 0.2$  for lime mortar and  $B = 0.25$  for all other cases were used  
548 for the analysis. As can be seen in Figs. 8e and 9e, results overestimate smaller  
549 strengths, probably because of the choice of parameter  $B$ . Furthermore, the  
550 model underestimates higher strengths, as already pointed out in [78].

551 Finally, the comparisons were carried out with the model proposed in the  
552 Australian Standard AS3700-18 [79]:

$$f_M = k_h k_m f_b^{0.5} \quad (18)$$

553 where  $f_M$  and  $f_b$  are characteristic strengths,  $k_h = \min[1.3, 1.3(19h_m/h_b)^{-0.29}]$   
554 is a joint thickness factor, and  $k_m$  is a compressive strength factor which for  
555 clay-masonry units and full bedding type it is equal to 1.1, 1.4, and 2.0 for  
556 mortar type M2, M3, and M4 respectively. Also in this case it is not easy to  
557 find a correspondence between the strength of mortar and its type, therefore it  
558 was decided to use  $k_m = 1.4$  for lime mortar and  $k_m = 2$  for all the other cases.  
559 In addition, the characteristic strength provided by Eq. 18 was multiplied by  
560 1.2 to obtain the average strength. For the compressive strength of bricks, the  
561 values reported in Tab. A2 were used. For consistency, the correction factor  
562 for slendernesses  $h_M/t_M < 5$  published by AS3700-18 has been used in place of  
563 ASTM 1314-18 to correct the experimental strengths.

564 Figs. 8f and 9f show the results for AS3700-18 [79] model. Also in this case  
565 the model seems to overestimate the lowest strengths and underestimate the  
566 highest ones.

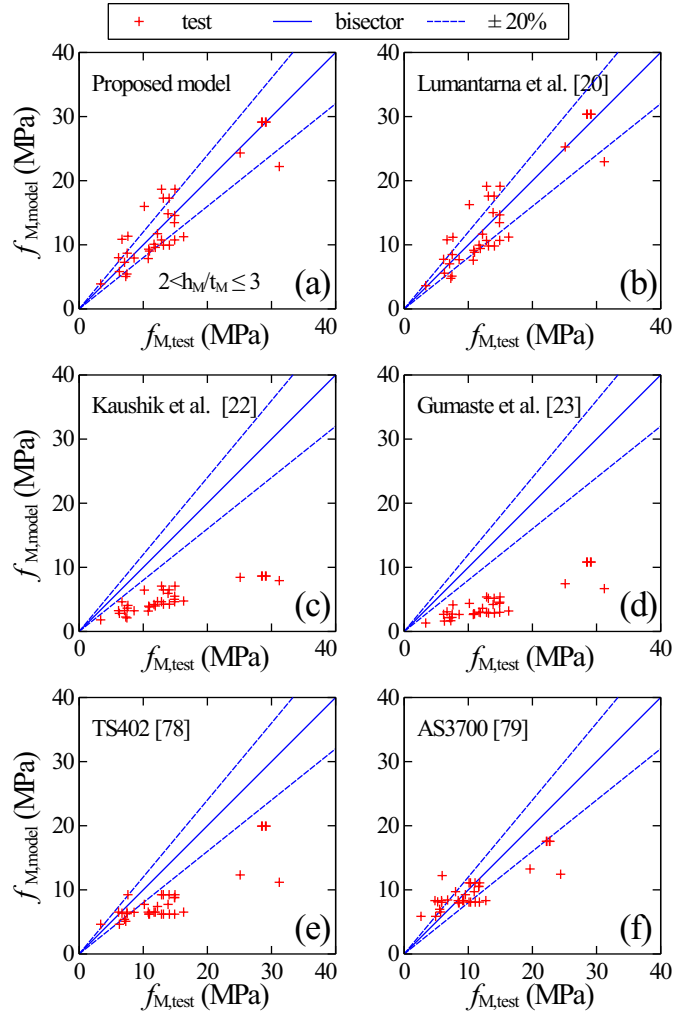


**Fig. 8:** Stack-bonded prisms with  $2 < h_m/t_m \leq 3$ . Comparison between experimental compressive strengths  $f_{M,test}$  and compressive strengths predicted by the calibrated model  $f_{M,model}$ : (a) Proposed model ; (b) Lumantarna et al. [20]; (c) Kaushik et al. [22] ; (d) Gumaste et al. [23]; (e) TMS402/602-16 [78]; (f) AS3700-18 [79].

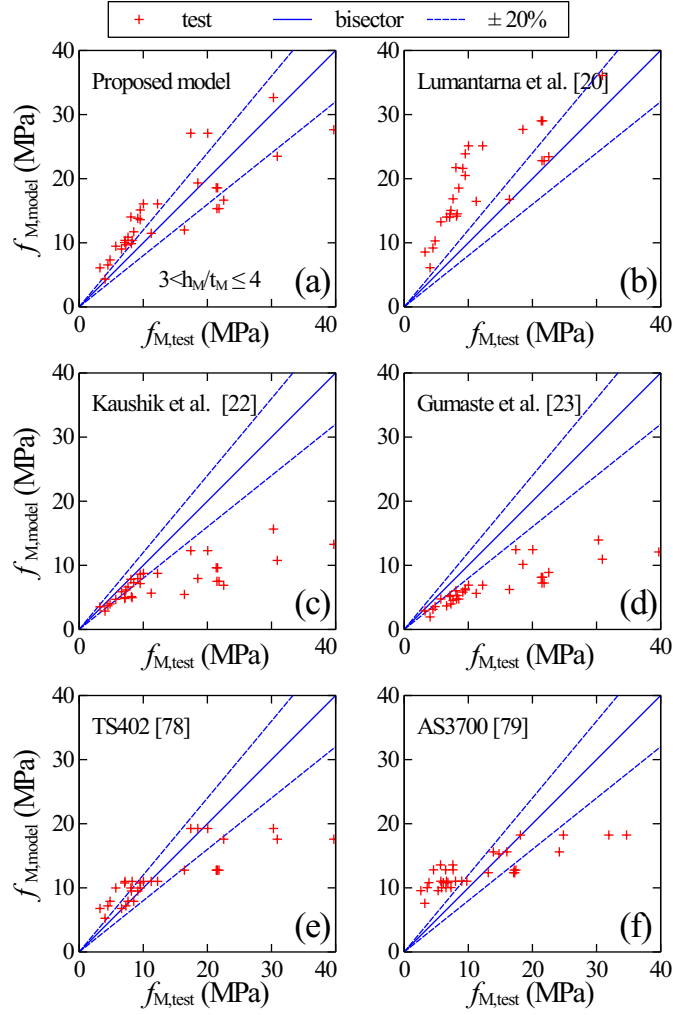


**Fig. 9:** Stack-bonded prisms with  $3 < h_m/t_m \leq 4$ . Comparison between experimental compressive strengths  $f_{M,test}$  and compressive strengths predicted by the calibrated model  $f_{M,model}$ : (a) Proposed model ; (b) Lumantarna et al. [20]; (c) Kaushik et al. [22] ; (d) Gumaste et al. [23]; (e) TMS402/602-16 [78]; (f) AS3700-18 [79].

Type	Model	all			cement-lime			lime		
		$R^2$	$a_{20}$	$AIC_c$	$R^2$	$a_{20}$	$AIC_c$	$R^2$	$a_{20}$	$AIC_c$
$2 \leq h_M/t_M < 3$	Proposed	0.82	0.54	86.10	0.57	0.50	62.59	0.24	0.38	24.87
	Lumantarna et al. [20]	0.81	0.46	90.79	0.52	0.36	67.90	0.11	0.38	-
	Kaushik et al. [22]	-1.03	0.00	174.06	-2.25	0.00	109.90	-2.52	0.00	-
	Gumaste et al. [23]	-1.16	0.00	173.64	-3.07	0.00	111.87	-3.53	0.00	39.20
	TMS402/602-16 [78]	0.18	0.14	139.86	-0.91	0.05	95.20	-0.38	0.38	29.71
	AS3700-18 [79]	0.63	0.49	94.58	0.34	0.59	61.07	-0.37	0.5	25.67
$3 \leq h_M/t_M < 4$	Proposed	0.74	0.21	114.33	0.70	0.23	95.03	-	-	-
	Lumantarna et al. [20]	-0.12	0.18	165.49	-0.06	0.23	131.17	-	-	-
	Kaushik et al. [22]	-0.01	0.27	162.03	-0.21	0.23	134.58	-	-	-
	Gumaste et al. [23]	-0.11	0.03	162.71	-0.32	0.00	133.95	-	-	-
	TMS402/602-16 [78]	0.44	0.45	140.42	0.34	0.50	116.09	-	-	-
	AS3700-18 [79]	0.44	0.21	125.79	0.47	0.27	98.99	-	-	-

**Table 8:** Comparison of the proposed model to the ones published in the literature: Stack-bonded prisms.

567 The different estimators for the quality of the models are reported in Tab. 8.  
568 Considering the coefficient of determination  $R^2$ , it is possible to notice that  
569 both for the proposed model and for Lumantarna’s model,  $R^2$  is about 0.8 if all  
570 the specimens are considered and slightly diminishes in the case of cement-lime  
571 mortar, also because of the scant number of points.

572 The models proposed by Kaushik et al. [22], Gumaste et al. [23], and  
573 TMS402/602-16 [78] are characterized by poor values of the coefficient of de-  
574 termination  $R^2$ , which in some cases are even negative (Tab. 8). In this case,  
575 the mean value of the strengths fits better the results than the model. Model  
576 AS3700-18 [79], on the other hand, provides slightly better results.

577 The proposed model presents also the best values of parameters  $AIC_c$  and  
578  $a_{20}$ , whereas the other models present poor values, similarly to what obtained  
579 in [14]. On the contrary, also for these parameters the model AS3700-18 [79]  
580 provides acceptable results.

581 In case of lime mortar, all the models show worse results than those obtained

582 for wallettes.

583 Results generally confirm that the models proposed in the literature repre-  
584 sent well the data used for their calibration but are not able to describe with  
585 accuracy the considered dataset, which is characterized by different dimension-  
586 less parameters. The AS3700-18 model is a separate case, presumably because it  
587 explicitly takes into account more dimensionless parameters (the slenderness of  
588 the specimens and the ratio between the thickness of the bed mortar joints and  
589 the block). The explicit inclusion of these and other dimensionless parameters  
590 is probably the way forward to generalize the power model, allowing a unified  
591 approach to compressive strength of masonry.

592 The proposed regressions are not intended to be, once again, just a calibra-  
593 tion of the power equation for the specific case (perhaps they are too many to be  
594 adopted in the codes). They rather permit to open a reflection on the adopted  
595 procedures and the uncertainties of the results.

## 596 **6. Conclusions**

597 The power equation is one of the most common phenomenological relation-  
598 ships used in the literature to forecast the compressive strength of masonry,  
599 which has been proposed with different coefficients and exponents by many  
600 authors. In the present work, the power equation was discussed by means of  
601 Dimensional Analysis. Nine dimensionless groups affecting masonry strength  
602 were introduced to identify and discuss the field of applicability of the power  
603 equation. Then, a dataset of 116 specimens selected from the literature was  
604 analyzed considering these dimensionless groups. Subsequently, experimental  
605 data were clustered considering the most significant dimensionless groups and  
606 used to calibrate new power equations for the different cases. Then, the new  
607 models were compared with some power models proposed in the literature. The  
608 results indicate that:

- 609 • It is proved from the theoretical point of view that the coefficients of the  
610 power equation must depend on the geometry of the specimens and on

611 the mechanical properties of the materials. For this reason, the power  
612 equations proposed in the literature are specific for the type of specimens  
613 (i.e. dimensionless parameters) used for their calibration and direct com-  
614 parisons among them should be done with great caution.

- 615 • A novel representation of the experimental data in the cartesian plane, in  
616 terms of dimensionless masonry strength (masonry efficiency) vs. dimen-  
617 sionless mortar strength, permits to observe the importance of specimen  
618 type (wallettes or stack-bonded prisms), specimen slenderness, and mortar  
619 type (cement, cement-lime, and lime). Furthermore, plots of the collected  
620 dataset show that the effect of slenderness is well evident for stack-bonded  
621 prism specimens and a suitable correction function should be studied.
- 622 • A new calibration of the power equation specific for solid-clay-brick ma-  
623 sonry was done considering homogeneous data in terms of dimensionless  
624 parameters. Compared to the power models proposed in the literature,  
625 the results of fitting are characterized by more consistent estimators. Re-  
626 gressions confirm once again that the power equations proposed in the  
627 literature are specific for the type of specimens (i.e. dimensionless param-  
628 eters) used for their calibration.
- 629 • The coefficient of determination  $R^2$  is insufficient to evaluate the quality of  
630 a regression. The combination of several estimators, like  $R^2$ , Akaike's In-  
631 formation Criterion, and  $a_{20}$  seems a good choice for the specific problem,  
632 providing more motivated judgments.

633 The application of the concepts of Dimensional Analysis is new in the field  
634 of masonry, where most (if not all) analyses are based on statistical treatment  
635 of the measured dimensional variables, with empirical or semi-empirical corre-  
636 lations.

637 Starting from a broad perspective on masonry compressive strength, the  
638 problem was narrowed to the simple case of the power equation. Also in this  
639 case the available experiments are by far not enough to perform a thorough

640 analysis in order to leave in place all the variables, hence only the most relevant  
641 can be saved. The detailed process of the selection is useful in order to perceive  
642 the approximations and the limits of the use of power equations for masonry  
643 strength.

644 The results of the present work are not intended to propose yet another  
645 calibration of the power equation but rather to allow a different reading and  
646 systematization of the problem, identifying better the context and its limits, and  
647 suggesting new developments with the aim of improving the overall approach  
648 to the problem.

#### 649 **Acknowledgements**

650 The Author thank Prof. Piero Ganugi and Prof. Marco Riani for the advices  
651 on statistics. Furthermore, Prof. Sandro Longo is gratefully acknowledged  
652 for the engaging discussions on dimensional analysis. Dr. Erica Lenticchia is  
653 gratefully acknowledged for many useful inputs and valuable comments.

654 This research did not receive any specific grant from funding agencies in the  
655 public, commercial, or not-for-profit sectors.



<b>N.</b>	<b>ref.</b>	$b_M \times t_M \times h_M$ (mm)	<b>wythes</b> (-)	$f_M$ (MPa)	$b_b \times t_b \times h_b$ (mm)	$f_b$ (MPa)	$f'_b$ (MPa)	$h_m$ (mm)	$f_m$ (MPa)	<b>mortar</b> (-)
1	[36]	500 × 250 × 600	2	11.00	250 × 120 × 55	26.90	21.52	10.00	3.20	l
2	[36]	500 × 250 × 600	2	14.50	250 × 120 × 55	26.90	21.52	10.00	12.70	c+l
3	[37]	442 × 103 × 385	1	5.69	215 × 103 × 65	12.00	10.14	12.00	4.39	l
4	[37]	442 × 103 × 385	1	6.32	215 × 103 × 65	12.00	10.14	12.00	7.02	l
5	[37]	442 × 103 × 385	1	1.53	215 × 103 × 65	12.00	10.14	12.00	0.89	l
6	[38]	500 × 115 × 370	1	9.50	250 × 115 × 55	26.40	22.44	10.00	4.70	l
7	[38]	500 × 115 × 370	1	9.40	250 × 115 × 55	26.40	22.44	10.00	5.80	l
8	[38]	500 × 115 × 370	1	12.90	250 × 115 × 55	26.40	22.44	10.00	9.80	c+l
9	[39]	520 × 110 × 350	1	5.40	— × 110 × —	15.20	12.92	-	5.80	l
10	[39]	520 × 110 × 350	1	8.80	— × 110 × —	15.20	12.92	-	9.80	c+l
11	[40]	280 × 140 × 300	1	8.14	280 × 140 × 55	19.70	16.74	8.00	2.30	l
12	[40]	280 × 140 × 300	1	7.42	280 × 140 × 55	19.70	16.74	8.00	2.30	l
13	[40]	280 × 140 × 300	1	6.14	280 × 140 × 55	19.70	16.74	8.00	2.30	l
14	[40]	280 × 140 × 300	1	7.47	280 × 140 × 55	19.70	16.74	8.00	2.30	l
15	[40]	280 × 140 × 300	1	8.50	280 × 140 × 55	19.70	16.74	8.00	2.30	l
16	[40]	280 × 140 × 300	1	7.60	280 × 140 × 55	19.70	16.74	8.00	2.30	l
17	[41]	660 × 200 × 800	2	1.79	200 × 100 × 70	7.82	6.81	15.00	1.04	l
18	[42]	430 × 100 × 330	1	4.64	200 × 100 × 50	10.00	10.00	-	3.33	c+l
19	[42]	430 × 100 × 330	1	7.14	200 × 100 × 50	32.00	32.00	-	2.87	c+l
20	[42]	430 × 100 × 330	1	10.41	200 × 100 × 50	32.00	32.00	-	9.84	c+l
21	[43]	500 × 120 × 500	1	14.98	250 × 120 × 65	17.40	17.40	13.00	13.85	c
22	[43]	500 × 120 × 500	1	12.51	250 × 120 × 65	17.40	17.40	13.00	9.47	c+l
23	[43]	500 × 120 × 500	1	6.93	250 × 120 × 65	17.40	17.40	13.00	1.13	l
24	[44]	380 × 260 × 590	2	6.60	250 × 120 × 50	15.70	15.70	-	11.10	c+l
25	[44]	380 × 260 × 590	2	8.30	250 × 120 × 50	21.20	21.20	-	10.60	c+l
26	[44]	380 × 260 × 590	2	10.80	250 × 120 × 50	27.20	27.20	-	10.40	c+l
27	[44]	380 × 260 × 590	2	5.60	250 × 120 × 50	16.30	16.30	-	5.80	c+l
28	[44]	380 × 260 × 590	2	8.00	250 × 120 × 50	22.20	22.20	-	6.20	c+l
29	[44]	380 × 260 × 590	2	9.80	250 × 120 × 50	28.30	28.30	-	5.50	c+l
30	[44]	380 × 260 × 590	2	9.60	250 × 120 × 50	28.50	28.50	-	5.80	c+l
31	[23]	235 × 115 × 460	1	13.60	235 × 111 × 76	23.00	20.08	12.00	12.21	c+l
32	[23]	235 × 115 × 460	1	6.70	235 × 111 × 76	23.00	20.08	12.00	6.60	c
33	[23]	235 × 115 × 460	1	12.60	235 × 111 × 76	23.00	20.08	12.00	12.21	c+l
34	[23]	235 × 115 × 460	1	9.60	235 × 111 × 76	23.00	20.08	12.00	6.60	c
35	[18]	700 × 230 × 700	2	5.40	230 × — × 70	13.10	13.10	10.00	6.10	c

Continued on next page

Table A1 – continued from previous page

N.	ref.	$b_M \times t_M \times h_M$ (mm)	wythes (-)	$f_M$ (MPa)	$b_b \times t_b \times h_b$ (mm)	$f_b$ (MPa)	$f'_b$ (MPa)	$h_m$ (mm)	$f_m$ (MPa)	mortar (-)
36	[45]	440 × 103 × 365	1	8.90	215 × 103 × 65	15.00	12.00	10.00	10.00	l
37	[45]	440 × 103 × 365	1	4.80	215 × 103 × 65	15.00	12.00	10.00	2.70	l
38	[45]	440 × 103 × 365	1	0.74	215 × 103 × 65	15.00	12.00	10.00	0.60	l
39	[45]	440 × 103 × 365	1	1.52	215 × 103 × 65	15.00	12.00	10.00	0.90	l
40	[45]	440 × 103 × 365	1	4.30	215 × 103 × 65	15.00	12.00	10.00	1.40	l
41	[45]	440 × 103 × 365	1	5.75	215 × 103 × 65	15.00	12.00	10.00	1.20	c

Table A1: Database of experimental values: wallettes.

N.	ref.	$b_M \times t_M \times h_M$ (mm)	$f_M$ (MPa)	$f'_M$ (MPa)	$b_b \times t_b \times h_b$ (mm)	$f_b$ (MPa)	$f'_b$ (MPa)	$h_m$ (mm)	$f_m$ (MPa)	mortar (-)
1	[46]	193 × 93 × 465	17.60	21.47	193 × 93 × 53	30.00	23.52	10.00	10.10	c+l
2	[47]	140 × 140 × 300	7.54	7.60	260 × 130 × 55	30.51	25.93	-	2.31	l
3	[48]	250 × 110 × 270	12.50	12.84	250 × 110 × 55	13.80	13.80	10.00	9.20	c+l
4	[48]	250 × 110 × 270	14.50	14.90	250 × 110 × 55	13.80	13.80	10.00	9.20	c+l
5	[48]	250 × 110 × 270	12.80	13.15	250 × 110 × 55	13.80	13.80	10.00	7.00	c+l
6	[48]	250 × 110 × 270	13.70	14.07	250 × 110 × 55	13.80	13.80	10.00	7.00	c+l
7	[40]	240 × 110 × 270	12.51	12.85	240 × 110 × 55	30.50	25.93	10.00	13.10	c+l
8	[40]	240 × 110 × 270	14.55	14.95	240 × 110 × 55	30.50	25.93	10.00	13.10	c+l
9	[40]	240 × 110 × 270	12.78	13.13	240 × 110 × 55	30.50	25.93	10.00	10.00	c+l
10	[40]	240 × 110 × 270	13.66	14.03	240 × 110 × 55	30.50	25.93	10.00	10.00	c+l
11	[49]	191 × 95 × 523	15.56	18.98	191 × 95 × -	34.00	34.00	-	15.70	c
12	[42]	200 × 100 × 330	3.69	4.04	200 × 100 × 50	10.00	10.00	-	3.33	c+l
13	[42]	200 × 100 × 330	6.49	7.10	200 × 100 × 50	32.00	32.00	-	2.87	c+l
14	[42]	200 × 100 × 330	8.70	9.52	200 × 100 × 50	32.00	32.00	-	9.84	c+l
15	[50]	285 × 130 × 280	28.90	29.17	285 × 130 × 50	56.80	68.73	10.00	5.50	c
16	[50]	285 × 130 × 280	28.80	29.07	285 × 130 × 50	56.80	68.73	10.00	5.50	c
17	[50]	285 × 130 × 280	28.20	28.46	285 × 130 × 50	56.80	68.73	10.00	5.50	c
18	[50]	285 × 130 × 280	28.30	28.56	285 × 130 × 50	56.80	68.73	10.00	5.50	c
19	[20]	228 × 112 × 250	3.31	3.36	228 × 112 × 78	8.50	7.50	15.00	1.23	l
20	[20]	228 × 112 × 250	6.98	7.08	228 × 112 × 78	12.00	10.58	15.00	4.54	c+l
21	[20]	228 × 112 × 250	10.70	10.85	228 × 112 × 78	15.70	13.85	15.00	5.53	l
22	[20]	228 × 112 × 250	7.39	7.49	228 × 112 × 78	16.00	14.11	15.00	4.14	c+l
23	[20]	228 × 112 × 250	6.59	6.68	228 × 112 × 78	16.30	14.38	15.00	8.58	l

Continued on next page

Table A2 – continued from previous page

N.	ref.	$b_M \times t_M \times h_M$ (mm)	$f_M$ (MPa)	$f'_M$ (MPa)	$b_b \times t_b \times h_b$ (mm)	$f_b$ (MPa)	$f'_b$ (MPa)	$h_m$ (mm)	$f_m$ (MPa)	mortar (–)
24	[20]	228 × 112 × 250	6.06	6.14	228 × 112 × 78	17.10	15.08	15.00	2.62	l
25	[20]	228 × 112 × 250	12.05	12.22	228 × 112 × 78	21.10	18.61	15.00	5.92	l
26	[20]	228 × 112 × 250	14.70	14.90	228 × 112 × 78	27.30	24.08	15.00	6.65	c+l
27	[20]	228 × 112 × 250	6.19	6.28	228 × 112 × 78	8.50	7.50	15.00	4.95	c+l
28	[20]	228 × 112 × 250	7.17	7.27	228 × 112 × 78	10.60	9.35	15.00	1.75	l
29	[20]	228 × 112 × 250	10.82	10.97	228 × 112 × 78	15.70	13.85	15.00	4.95	c+l
30	[20]	228 × 112 × 250	7.35	7.45	228 × 112 × 78	17.10	15.08	15.00	0.69	l
31	[20]	228 × 112 × 250	10.63	10.78	228 × 112 × 78	17.10	15.08	15.00	2.47	c+l
32	[20]	228 × 112 × 250	11.71	11.87	228 × 112 × 78	17.10	15.08	15.00	4.95	c+l
33	[20]	228 × 112 × 250	11.52	11.68	228 × 112 × 78	17.10	15.08	15.00	5.90	c+l
34	[20]	228 × 112 × 250	16.07	16.29	228 × 112 × 78	17.10	15.08	15.00	8.65	c+l
35	[20]	228 × 112 × 250	14.66	14.86	228 × 112 × 78	27.50	24.25	15.00	4.95	c+l
36	[20]	228 × 112 × 250	30.79	31.22	228 × 112 × 78	38.20	33.69	15.00	12.52	c+l
37	[20]	228 × 112 × 250	24.77	25.12	228 × 112 × 78	43.40	38.28	15.00	12.52	c+l
38	[23]	235 × 115 × 460	6.70	7.70	235 × 111 × 76	23.00	20.08	12.00	6.60	c
39	[51]	240 × 110 × 270	9.90	10.17	240 × 110 × 55	19.90	19.90	10.00	14.72	c+l
40	[51]	240 × 110 × 270	13.50	13.87	240 × 110 × 55	19.90	19.90	10.00	11.39	c+l
41	[52]	230 × 110 × 400	4.00	4.48	230 × 110 × 75	17.70	17.70	10.00	3.10	c
42	[52]	230 × 110 × 400	2.90	3.25	230 × 110 × 75	16.10	16.10	10.00	3.10	c
43	[52]	230 × 110 × 400	5.10	5.72	230 × 110 × 75	28.90	28.90	10.00	3.10	c
44	[52]	230 × 110 × 400	4.30	4.82	230 × 110 × 75	20.60	20.60	10.00	3.10	c
45	[52]	230 × 110 × 400	8.50	9.53	230 × 110 × 75	28.90	28.90	10.00	20.60	c
46	[52]	230 × 110 × 400	7.60	8.52	230 × 110 × 75	20.60	20.60	10.00	20.60	c
47	[52]	230 × 110 × 400	6.50	7.29	230 × 110 × 75	17.70	17.70	10.00	15.20	c+l
48	[52]	230 × 110 × 400	5.90	6.61	230 × 110 × 75	16.10	16.10	10.00	15.20	c+l
49	[52]	230 × 110 × 400	7.20	8.07	230 × 110 × 75	28.90	28.90	10.00	15.20	c+l
50	[52]	230 × 110 × 400	6.80	7.62	230 × 110 × 75	20.60	20.60	10.00	15.20	c+l
51	[6]	194 × 89 × 350	37.70	43.15	194 × 89 × 55	69.80	59.33	7.50	52.60	c+l
52	[6]	194 × 89 × 350	34.70	39.72	194 × 89 × 55	69.80	59.33	7.50	26.40	c+l
53	[6]	194 × 89 × 350	27.00	30.90	194 × 89 × 55	69.80	59.33	7.50	13.70	c+l
54	[6]	194 × 89 × 350	19.70	22.55	194 × 89 × 55	69.80	59.33	7.50	3.40	c+l
55	[53]	250 × 120 × 315	8.24	8.57	250 × 120 × 55	19.76	14.95	10.00	2.62	c
56	[54]	210 × 100 × 340	27.50	30.30	204 × 98 × 50	66.00	66.00	14.00	37.50	l
57	[54]	430 × 100 × 340	18.20	20.06	204 × 98 × 50	66.00	66.00	14.00	17.60	c+l

Continued on next page

Table A2 – continued from previous page

N.	ref.	$b_M \times t_M \times h_M$ (mm)	$f_M$ (MPa)	$f'_M$ (MPa)	$b_b \times t_b \times h_b$ (mm)	$f_b$ (MPa)	$f'_b$ (MPa)	$h_m$ (mm)	$f_m$ (MPa)	mortar (–)
58	[54]	210 × 100 × 340	15.80	17.41	204 × 98 × 50	66.00	66.00	14.00	17.60	c+1
59	[54]	210 × 100 × 340	8.30	9.15	212 × 99 × 51	27.00	27.00	14.00	17.60	c+1
60	[54]	430 × 100 × 340	11.10	12.23	208 × 98 × 50	33.00	33.00	14.00	17.60	c+1
61	[54]	210 × 100 × 340	9.10	10.03	208 × 98 × 50	33.00	33.00	14.00	17.60	c+1
62	[54]	430 × 100 × 340	19.40	21.38	212 × 100 × 53	40.00	40.00	14.00	17.60	c+1
63	[54]	430 × 100 × 340	19.60	21.60	212 × 100 × 53	40.00	40.00	14.00	17.60	c+1
64	[54]	210 × 100 × 340	16.80	18.51	208 × 98 × 50	66.00	66.00	15.00	4.50	c+1
65	[54]	210 × 100 × 340	7.40	8.15	212 × 99 × 51	27.00	27.00	14.00	4.50	c+1
66	[54]	210 × 100 × 340	10.20	11.24	208 × 98 × 50	33.00	33.00	14.00	4.50	c+1
67	[54]	430 × 100 × 340	19.80	21.82	212 × 100 × 53	40.00	40.00	12.50	8.10	c+1
68	[54]	430 × 100 × 340	19.50	21.49	212 × 100 × 53	40.00	40.00	12.50	8.10	c+1
69	[54]	430 × 100 × 340	7.50	8.26	208 × 98 × 50	33.00	33.00	14.00	3.00	c+1
70	[54]	210 × 100 × 340	6.50	7.16	208 × 98 × 50	33.00	33.00	14.00	3.00	c+1
71	[54]	430 × 100 × 340	14.90	16.42	212 × 100 × 53	40.00	40.00	14.00	3.00	c+1
72	[55]	290 × 140 × 273	12.30	12.13	290 × 140 × 50	21.30	17.04	10.00	1.23	1
73	[55]	290 × 140 × 265	11.78	11.43	290 × 140 × 50	21.30	17.04	10.00	1.23	1
74	[55]	290 × 140 × 265	13.80	13.39	290 × 140 × 50	21.30	17.04	10.00	1.90	1
75	[55]	290 × 140 × 268	13.66	13.33	290 × 140 × 50	21.30	17.04	10.00	1.90	1

Table A2: Database of experimental values: stack-bonded prisms.

657 **References**

- 658 [1] Engesser F. Über weitgespannte wölbbrücken. Zeitschrift für Architekturs  
659 und Ingenieurwesen 1907;53:403–40.
- 660 [2] Circolare n. 7/19 . Istruzioni per l’applicazione dell’aggiornamento delle  
661 norme tecniche per le costruzioni di cui al D.M. 17 gennaio 2018, G.U. n.  
662 35/2019. Ministero delle Infrastrutture e dei Trasporti; (in Italian); 2019.
- 663 [3] Dymiotis C, Gutleiderer BM. Allowing for uncertainties in the modelling of  
664 masonry compressive strength. Constr Build Mater 2002;16(8):443–52.
- 665 [4] Garzón-Roca J, Marco CO, Adam JM. Compressive strength of masonry  
666 made of clay bricks and cement mortar: Estimation based on neural net-  
667 works and fuzzy logic. Eng Struct 2013;48:21–7.
- 668 [5] Hendry AW. Structural masonry. Palgrave Macmillan; 2nd ed.; 1998.
- 669 [6] McNary WS, Abrams DP. Mechanics of masonry in compression. J Struct  
670 Eng-ASCE 1985;111(4):857–70.
- 671 [7] Haller P, Sinclair DA. The technological properties of brick masonry in  
672 high buildings. Canada NRC Technical Translation Tt; National Research  
673 Council of Canada, Division of Building Research; 1959.
- 674 [8] Biolzi L. Evaluation of compressive strength of masonry walls by limit  
675 analysis. J Struct Eng-ASCE 1988;114(10):2179–89.
- 676 [9] Uday Vyas C, Venkatarama Reddy B. Prediction of solid block masonry  
677 prism compressive strength using FE model. Mater Struct 2010;43(5):719–  
678 35.
- 679 [10] Lourenço PB, Pina-Henriques J. Validation of analytical and continuum  
680 numerical methods for estimating the compressive strength of masonry.  
681 Comput Struct 2006;84(29):1977–89.

- 682 [11] Drougkas A, Roca P, Molins C. Numerical prediction of the behavior,  
683 strength and elasticity of masonry in compression. *Eng Struct* 2015;90:15–  
684 28.
- 685 [12] Zahra T, Dhanasekar M. Prediction of masonry compressive behaviour  
686 using a damage mechanics inspired modelling method. *Constr Build Mater*  
687 2016;109:128–38.
- 688 [13] Thamboo J, Dhanasekar M. Nonlinear finite element modelling of high  
689 bond thin-layer mortared concrete masonry. *International Journal of Ma-*  
690 *sonry Research and Innovation* 2016;1(1):5–26.
- 691 [14] Asteris PG, Argyropoulos I, Cavaleri L, Rodrigues H, Varum H, Thomas  
692 J, et al. Masonry compressive strength prediction using artificial neural  
693 networks. In: Moropoulou A, Korres M, Georgopoulos A, Spyrakos C,  
694 Mouzakis C, editors. *Proc. of the 1st Int. Conf. TMM-CH, Transdisci-*  
695 *plinary Multispectral Modelling and Cooperation for the Preservation of*  
696 *Cultural Heritage, Athens, Greece, October 10-13, 2018.* Springer; 2019, p.  
697 10–3.
- 698 [15] Ferretti D, Coisson E, Ugolotti D, Lenticchia E. Use of EC6-like equations  
699 to estimate the compressive strength of masonry made of solid clay bricks  
700 and lime mortar. In: Modena C, da Porto F, Valluzzi M, editors. *Proc.*  
701 *of the 16th Int. Brick and Block Masonry Conference, Padova, Italy, 26-30*  
702 *June 2016.* Taylor & Francis Group, London; 2016, p. 1561–70.
- 703 [16] Liberatore D, Marotta A, Sorrentino L. Estimation of clay-brick unrein-  
704 forced masonry compressive strength based on mortar and unit mechanical  
705 parameters. In: Lourenço PB, Haseltine B, Vasconcelos G, editors. *Proc. of*  
706 *9th International Conference of Masonry, Guimarães, Portugal, 07-09 July*  
707 *2014.* 2014, p. 1–12.
- 708 [17] Eurocode 6 . EN 1996-1-1:2005: Design of masonry structures - Part 1-1:  
709 General rules for reinforced and unreinforced masonry structures. 2005.

- 710 [18] Malek MH. Compressive strength of brickwork masonry with special ref-  
711 erence to concentrated load. Ph.D. thesis; Dept. of Civil Engrg. and Civil  
712 Sciences, University of Edimburgh; 1987.
- 713 [19] Hendry AW, Malek MH. Characteristic compressive strength of brickwork  
714 walls from collected test results. *Masonry Int* 1986;7:15–24.
- 715 [20] Lumantarna R, Biggs DT, Ingham JM. Uniaxial compressive strength and  
716 stiffness of field extracted and laboratory constructed masonry prisms. *J*  
717 *Mater Civil Eng* 2014;26(4):567–75.
- 718 [21] Mann W. Statistical evaluation of tests on masonry by potential functions.  
719 In: Proc. of the 6th International Brick Masonry Conference, ROME, Italy,  
720 16-19 May 1982. (in German): ANDIL; 1982, p. 77–83.
- 721 [22] Kaushik HB, Rai DC, Jain SK. Stress-strain characteristics of clay brick  
722 masonry under uniaxial compression. *J Mater Civil Eng* 2007;19(9):728–39.
- 723 [23] Gumaste KS, Rao KSN, Reddy BVV, Jagadish KS. Strength and elasticity  
724 of brick masonry prisms and wallettes under compression. *Mater Struct*  
725 2007;40(2):241–53.
- 726 [24] Dayaratnam P. Brick and reinforced brick structures. South Asia Books;  
727 1987.
- 728 [25] Barenblatt GI. Scaling, self-similarity, and intermediate asymptotics: di-  
729 mensional analysis and intermediate asymptotics (Cambridge Texts in  
730 Applied Mathematics). Cambridge University Press; 1996. ISBN 978-  
731 0521435222.
- 732 [26] Szirtes T. Applied dimensional analysis and modeling. Butterworth-  
733 Heinemann; 2007. ISBN 0123706203.
- 734 [27] Longo S. Analisi dimensionale e modellistica fisica. Springer Milan (in  
735 Italian); 2011. ISBN 8847018714.

- 736 [28] Thaickavil NN, Thomas J. Behaviour and strength assessment of ma-  
737 sonry prisms. *Case Studies in Construction Materials* 2018;8:23–38. doi:  
738 10.1016/j.cscm.2017.12.007.
- 739 [29] Grimm CT. Strength and related properties of brick masonry. *Journal of*  
740 *the Structural Division* 1975;101(1):217–32.
- 741 [30] fib Federation Internationale du Beton . *fib Model Code for Concrete*  
742 *Structures* 2010. Ernst W. + Sohn Verlag; 2013. ISBN 3433030618.
- 743 [31] Caporale A, Parisi F, Asprone D, Luciano R, Prota A. Comparative mi-  
744 cromechanical assessment of adobe and clay brick masonry assemblages  
745 based on experimental data sets. *Compos Struct* 2015;120:208–20. doi:  
746 10.1016/j.compstruct.2014.09.046.
- 747 [32] Sonin AA. A generalization of the  $\Pi$ -theorem and dimensional analy-  
748 sis. *Proc of the National Academy of Sciences* 2004;101(23):8525–6. doi:  
749 10.1073/pnas.0402931101.
- 750 [33] Zucchini A, Lourenço PB. Mechanics of masonry in compression: Results  
751 from a homogenisation approach. *Comput Struct* 2007;85(3-4):193–204.
- 752 [34] Augenti N, Parisi F, Acconcia E. Mada: online experimental database  
753 for mechanical modelling of existing masonry assemblages. In: *Proc. of*  
754 *the 15th World Conference on Earthquake Engineering, Lisbon, Portugal,*  
755 *24-28 Sept 2012. SPES; 2012, p. 24–8.*
- 756 [35] Sarangapani G, Venkatarama Reddy BV, Jagadish KS. Brick-mortar bond  
757 and masonry compressive strength. *J Mater Civil Eng* 2005;17(2):229–37.
- 758 [36] Binda L, Fontana A, Frigerio G. Mechanical behaviour of brick masonries  
759 derived from unit and mortar characteristics. In: Courcy JWD, editor.  
760 *Proc. of the 8th Int. Brick and Block Masonry Conference, 19-21 Sept*  
761 *1988, Trinity College, Dublin; vol. 1. Elsevier Applied Science; 1988, p.*  
762 *205–16.*

- 763 [37] Costigan A, Pavía S. Compressive, flexural and bond strength of brick/lime  
764 mortar masonry. In: Mazzolani F, editor. Proc. of International Conference  
765 on Protection of Historical Buildings PROHITECH09, Rome, Italy, 21-24  
766 June 2009. CRC Press; 2009, p. 1609–15.
- 767 [38] Mattone R, Pasero G, Pavano M, Pistone G, Roccati R. Prove sperimentali  
768 su campioni di varie dimensioni volte alla determinazione delle caratteris-  
769 tiche meccaniche delle vecchie murature. In: Proc. of the 6th Int. Brick  
770 Masonry Conference, Rome 16-19 May 1982, (in Italian). ANDIL; 1982, p.  
771 198–209.
- 772 [39] Pistone G, Roccati R. Mechanical characteristics of masonry rebuilt with  
773 ancient bricks and fresh mortars. In: Proc. of the 9th Int. Brick & Block  
774 Masonry Conference, Berlin, Germany, 13-16 Oct 1991. Berlin: Deutsche  
775 Gesellschaft für Mauerwerksbau; 1991, p. 1473–80.
- 776 [40] Brencich A, de Felice G. Brickwork under eccentric compression:  
777 Experimental results and macroscopic models. Constr Build Mater  
778 2009;23(5):1935–46.
- 779 [41] Ignatakis C, Stylianides K. Mechanical characteristics of virgin and  
780 strengthened old brick masonry- experimental research. Masonry Int  
781 2004;17(1):9–17.
- 782 [42] Vermeltfoort AT. Mechanical properties under compression of masonry  
783 and its components. In: Proc. of the 6th Canadian Masonry Symposium.  
784 1992, p. 657–62.
- 785 [43] Bosiljkov V. Micro vs. macro reinforcement of brickwork masonry. Mater  
786 Struct 2006;39(2):235–45.
- 787 [44] Zago F, Riva G. Proprietà fisico-meccaniche dei mattoni e comportamento  
788 della muratura del centro storico di Venezia. Parte seconda: la muratura.  
789 Scuola Tipografica Emiliana Artigianelli, Venice, (in Italian) 1982;45:1–23.

- 790 [45] Costigan A, Pavía S, Kinnane O. An experimental evaluation of prediction  
791 models for the mechanical behavior of unreinforced lime-mortar masonry  
792 under compression. *Journal of Building Engineering* 2015;4:283–94.
- 793 [46] Maurenbrecher AHP. Effect of test procedures on compressive strength  
794 of masonry prisms. In: *Proc. of the 2nd Canadian Masonry Symposium*.  
795 Ottawa; 1980, p. 119–32.
- 796 [47] de Felice G. Experimental investigation on historic brickwork subjected  
797 to eccentric axial loads. In: *Proc. of the 5th Int. Conf. on Structural  
798 Analysis of Historical Constructions SAHC06*. Macmillan India Ltd New  
799 Delhi,, India; 2006, p. 809–16.
- 800 [48] Brencich A, Corradi C, Gambarotta L. Eccentrically loaded brickwork:  
801 Theoretical and experimental results. *Eng Struct* 2008;30(12):3629–43.
- 802 [49] Ewing BD, Kowalsky MJ. Compressive behavior of unconfined and confined  
803 clay brick masonry. *J Struct Eng-ASCE* 2004;130(4):650–61.
- 804 [50] Oliveira DV, Lourenço PB, Roca P. Cyclic behaviour of stone and brick  
805 masonry under uniaxial compressive loading. *Mater Struct* 2006;39(2):247–  
806 57.
- 807 [51] Brencich A, Gambarotta L. Mechanical response of solid clay brick-  
808 work under eccentric loading. Part I: Unreinforced masonry. *Mater Struct*  
809 2005;38(2):257–66.
- 810 [52] Kaushik HB, Durgesh CR, Sudhir KJ. Uniaxial compressive stress-strain  
811 model for clay brick masonry. *Current Science* 2007;92(4):497–501.
- 812 [53] Panizza M, Garbin E, Valluzzi MR, Modena C. Experimental investigation  
813 on bond of FRP/SRP applied to masonry prisms. In: *Proc. of 6th Int.  
814 Conference on FRP Composites in Civil Engineering (CICE 2012)*, 13-15  
815 June 2012, Rome, Italy. 2012, p. 1–8.

- 816 [54] Vermeltfoort A, Martens D, Van Zijl G. Brick-mortar interface effects on  
817 masonry under compression. *Can J Civil Eng* 2007;34(11):1475–85.
- 818 [55] Drougkas A, Roca P, Molins C. Compressive strength and elasticity of pure  
819 lime mortar masonry. *Mater Struct* 2016;49(3):983–99.
- 820 [56] Thamboo JA, Dhanasekar M. Correlation between the performance of  
821 solid masonry prisms and wallettes under compression. *Journal of Building*  
822 *Engineering* 2019;22:429–38.
- 823 [57] EN 1052-1:1998 . Methods of test for masonry: Determination of compres-  
824 sive strength. 1998.
- 825 [58] ASTM1314-14 . Standard Test Method for Compressive Strength of Ma-  
826 sonry Prisms - C1314-14. West Conshohocken, PA.: ASTM International;  
827 2014.
- 828 [59] Binda L, Mirabella Roberti G, Tiraboschi C. Problemi di misura dei  
829 parametri meccanici della muratura e dei suoi componenti. In: *Proc. of La*  
830 *meccanica delle murature tra teoria e progetto*, 18-20 Sept. 1996, Messina  
831 (Italy) (In Italian). 1996, p. 45–56.
- 832 [60] EN 772-1:2000 . Methods of test for masonry units Part 1: determination  
833 of compressive strength. 2011.
- 834 [61] Zhou Q, Wang F, Zhu F. Estimation of compressive strength of hol-  
835 low concrete masonry prisms using artificial neural networks and adap-  
836 tive neuro-fuzzy inference systems. *Constr Build Mater* 2016;125:417–26.  
837 doi:<http://dx.doi.org/10.1016/j.conbuildmat.2016.08.064>.
- 838 [62] Sarhat SR, Sherwood EG. The prediction of compressive strength of un-  
839 grouted hollow concrete block masonry. *Constr Build Mat* 2014;58:111–21.  
840 doi:<http://dx.doi.org/10.1016/j.conbuildmat.2014.01.025>.
- 841 [63] Lumantarna R. Material characterisation of New Zealand’s clay brick un-  
842 reinforced masonry buildings. Ph.D. thesis; The University of Auckland  
843 Department of Civil and Environmental Engineering; New Zealand; 2012.

- 844 [64] Antonelli C. Risultati di esperimenti eseguiti sulla resistenza alla com-  
845 pressione di alcuni pilastri in muratura. *L'Ingegneria Civile e le Arti*  
846 *Industriali*, (in Italian) 1885;11(1):1–5.
- 847 [65] Krefeld WJ. The effect of shape of specimens on the apparent compressive  
848 strength of brick masonry. *ASTM Proceedings* 1938;38(1):363–9.
- 849 [66] Noland JL, Hanada KT, Feng CC. The effect of slenderness and end co-  
850 efficients on the strength of clay unit prisms. In: *Proc. of the 1st North*  
851 *American Masonry Conference*. 1978, p. 14–1–14–27.
- 852 [67] Kingsley GR, Noland JL, Shuller MP. The effect of slenderness and end  
853 restraint on the behavior of masonry prisms: a literature review. *TMS*  
854 *Journal* 1992;10:31–47.
- 855 [68] Hamid AA, Chukwunenye AO. Compression behavior of concrete masonry  
856 prisms. *Journal of Structural Engineering* 1986;112(3):605–13.
- 857 [69] Fahmy EH, Ghoneim TGM. Behaviour of concrete block masonry  
858 prisms under axial compression. *Canadian Journal of Civil Engineering*  
859 1995;22(5):898–915.
- 860 [70] Korany Y, Glanville J. Comparing masonry compressive strength in various  
861 codes. *Concrete international* 2005;27(7):35–9.
- 862 [71] Hassanli R, ElGawady MA, Mills JE. Effect of dimensions on the compres-  
863 sive strength of concrete masonry prisms. *Advances in Civil Engineering*  
864 *Materials* 2015;4(1).
- 865 [72] Mathworks . *Statistics and Machine Learning Toolbox*; 2016. URL  
866 <http://www.mathworks.com/help/stats/index.html>.
- 867 [73] Riani M, Perrotta D, Torti F. *Fsda: A matlab toolbox for robust analysis*  
868 *and interactive data exploration. Chemometrics and Intelligent Laboratory*  
869 *Systems* 2012;116:17–32.

- 870 [74] Carino NJ. Statistical methods to evaluate in-place test results. ACI Special  
871 Publication 1993;141:39–64.
- 872 [75] ACI 228.1 R-03 . In-place methods to estimate concrete strength. ACI  
873 Committee 228; 2003.
- 874 [76] Mandel J. Fitting straight lines when both variables are subject to error.  
875 J Qual Technol 1984;16(1):1–14.
- 876 [77] Anderson D, Burnham K. Model selection and multi-model inference. NY:  
877 Springer-Verlag; 2nd ed.; 2004.
- 878 [78] TMS 402/602-16 . Building Code Requirements and Specifications for Ma-  
879 sonry Structures. 2016.
- 880 [79] AS3800:18 . Masonry Structures. Australian Standard; 2018.

881 **Notes**